

***A posteriori* error analysis for random scalar conservation laws using the stochastic Galerkin method**

FABIAN MEYER* AND CHRISTIAN ROHDE

*Institute of Applied Analysis and Numerical Simulation, University of Stuttgart, Pfaffenwaldring 57,
70569 Stuttgart, Germany*

*Corresponding author: fabian.meyer@mathematik.uni-stuttgart.de

AND

JAN GIesselmann

Department of Mathematics, TU Darmstadt, Dolivostraße 15, 64293 Darmstadt, Germany

[Received on 11 May 2018; revised on 11 October 2018]

In this article we present an *a posteriori* error estimator for the spatial–stochastic error of a Galerkin-type discretization of an initial value problem for a random hyperbolic conservation law. For the stochastic discretization we use the stochastic Galerkin method and for the spatial–temporal discretization of the stochastic Galerkin system a Runge–Kutta discontinuous Galerkin method. The estimator is obtained using smooth reconstructions of the discrete solution. Combined with the relative entropy stability framework of Dafermos (2016, *Hyperbolic Conservation Laws in Continuum Physics*, 4th edn., Grundlehren der Mathematischen Wissenschaften [Fundamental Principles of Mathematical Sciences], vol. 325, Berlin, Springer, pp. xxxviii+826), this leads to computable error bounds for the space–stochastic discretization error. Moreover, it turns out that the error estimator admits a splitting into one part representing the spatial error, and a remaining term, which can be interpreted as the stochastic error. This decomposition allows us to balance the errors arising from spatial and stochastic discretization. We conclude with some numerical examples confirming the theoretical findings.

Keywords: hyperbolic conservation laws; random pdes; *a posteriori* error estimates; stochastic Galerkin method; discontinuous Galerkin method; relative entropy.

1. Introduction

In numerical simulations, accounting for uncertainties in input quantities has become an important issue in recent decades. The two main sources for uncertainties are the limitations in measuring physical parameters exactly and the absence of knowledge of the underlying physical processes. Therefore, a whole new field of research, uncertainty quantification, has evolved in recent years. It addresses the question of how much we can rely on highly accurate numerical solutions if there are uncertain parameters.

For the quantification of uncertainties, there exist two major approaches. On the one hand, statistical approaches such as Monte Carlo-type methods sample the random space to obtain statistical information, like mean, variance or higher-order moments of the corresponding random field. On the other hand, nonstatistical approaches, like the intrusive and nonintrusive polynomial chaos expansion, approximate the random field by a series of polynomials and derive deterministic models for the stochastic modes.

The theoretical foundation for the polynomial chaos expansion was laid in Wiener (1938) and can be described as a polynomial approximation of Gaussian random variables to represent random processes. Later, the approach was generalized to a broader class of distributions. Xiu & Karniadakis (2002) considered polynomials from the so-called Askey scheme, where the approximating polynomials are orthonormal polynomials with respect to an inner product induced by the corresponding probability density function of the chosen probability distribution. The intrusive spectral projection, also known as the stochastic Galerkin (SG) approach, considers a weak formulation of the partial differential equation with respect to the stochastic variable and uses the corresponding orthonormal polynomials as ansatz and test functions. Compared to elliptic and parabolic equations (Ghanem & Spanos, 1991; Yan, 2005; Hoang & Schwab, 2013) the development of the SG method for hyperbolic equations faces additional problems. From an analytical point of view (nonlinear) elliptic and parabolic equations are better understood than (nonlinear) hyperbolic equations. Moreover, solutions of nonlinear hyperbolic equations may develop shocks (discontinuities) in finite time and these shocks also propagate into the stochastic space; cf. Le Maître *et al.* (2004). Another problem is the possible loss of hyperbolicity of the resulting SG system (Després *et al.*, 2013). Therefore, new approaches to treat these problems have to be developed. For an overview of recent work on uncertainty quantification for hyperbolic equations see Le Maître & Knio (2010), Bijl *et al.* (2013) and Pettersson *et al.* (2015). New numerical schemes for the SG system can be found in Wan & Karniadakis (2006), Bürger *et al.* (2014) and Jin & Ma (2018) and for the convergence analysis of approximate solutions of the SG system see Gottlieb & Xiu (2008), Zhou & Tang (2012) and Hu *et al.* (2015). However, in all these works the dimension of the discrete stochastic space is chosen in an *ad hoc* way, in particular independent of the spatial–temporal resolution. Space–stochastic adaptive schemes, based on heuristic indicators, are treated in Tryoen *et al.* (2012) and Kröker *et al.* (2015). A more reliable link between stochastic and space-time resolution can be provided by an appropriate *a posteriori* error estimator.

For the *a posteriori* analysis of deterministic scalar conservation laws, rigorous approaches accompanied with corresponding adaptive algorithms can be found in Gosse & Makridakis (2000) and Kröner & Ohlberger (2000); see also Cockburn (2003) and Dedner *et al.* (2007) and the references therein. These estimates were derived by exploiting Kružkov’s estimates. A different approach for the *a posteriori* analysis uses reconstructions of the discrete solutions to estimate the error in a suitable energy norm: cf. Georgoulis *et al.* (2014), or in the L^2 -norm Giesselmann *et al.* (2015) and Dedner & Giesselmann (2016). The approach in Dedner & Giesselmann (2016) combines the reconstruction of the discrete solutions with the relative entropy framework in Dafermos (2016). In contrast to Kružkov’s scalar theory, this approach is also applicable for hyperbolic systems that are endowed with a strictly convex entropy/entropy flux pair.

While there exists a rather firm theory for the *a posteriori* analysis of random elliptic and parabolic equations in combination with the SG method (Deb *et al.*, 2001; Mathelin & Le Maître, 2007; Butler *et al.*, 2011; Eigel *et al.*, 2014; Pultarová, 2015), the *a posteriori* analysis for hyperbolic problems is less developed. Besides the missing *a posteriori* analysis, most applications of the SG method for hyperbolic equations are rather *ad hoc*, in the sense that the resolution in the stochastic space is rather arbitrary and, in particular, not related to resolution in space and time. We address exactly this issue and, in particular, provide *a posteriori* error control in the form of a computable upper bound for the ‘overall’, i.e. spatio-temporal and stochastic, error. Moreover, the derived error estimator splits into two parts. One part quantifies errors caused by discretizing stochastic space while the other part quantifies errors due to discretization of time and physical space. This allows a precise tuning of the stochastic discretization with respect to the space-time discretization.

We study uncertainty in hyperbolic conservation laws resulting from uncertain initial data, parametrized by absolutely continuous random variables or random source terms. The main contribution of this paper is an *a posteriori* error estimator for a class of numerical schemes. In the schemes under consideration the random conservation law is discretized in stochastic space by the SG method. The resulting deterministic SG system is then numerically solved by a Runge–Kutta discontinuous Galerkin (DG) method. Our *a posteriori* analysis follows the approach in [Dedner & Giesselmann \(2016\)](#) in that it makes use of a space-time stochastic reconstruction of the discrete solutions. It turns out that this reconstruction satisfies a perturbed version of the original random conservation law with computable residual, so that the relative entropy framework allows us to prove a computable upper bound for the space-stochastic error. This upper bound is the main result of this paper (Theorem 3.8). The resultant estimator is valid also for discontinuous solutions, but it is only bounded as long as solutions are Lipschitz continuous. A particular feature of our analysis is that the corresponding residual admits an orthogonal decomposition into a stochastic residual and a spatial residual (Theorem 3.12). This splitting enables us to determine whether the overall error is dominated by the stochastic error, or the spatial error and thus, whether we should increase resolution in stochastic space, or refine in physical space to efficiently decrease the overall error. Furthermore, our *a posteriori* analysis complements the *a priori* analysis in [Gottlieb & Xiu \(2008\)](#) and [Hu et al. \(2015\)](#), where the authors proved spectral convergence of the approximate solutions of the SG system. In our numerical experiments the stochastic residual converges spectrally, i.e. our estimator for the SG-discretization error converges in the same way as the SG-discretization error according to the findings of [Gottlieb & Xiu \(2008\)](#) and [Hu et al. \(2015\)](#).

The outline of this work is as follows. In Section 2 we recall the notion of random entropy solutions and give a short introduction to the SG method. In Section 3 we describe how to reconstruct the numerical solutions for fully discrete SG DG schemes. Furthermore, we show how to construct so-called space-time stochastic reconstructions for the random scalar conservation law. We then prove the above-mentioned *a posteriori* error estimate and the orthogonal decomposition. Finally, in Section 4 we present numerical experiments illustrating the scaling behavior of the two parts of the space-stochastic residual.

2. Notation and preliminaries

Let $(\Omega, \mathcal{F}, \mathbb{P})$ be a probability space, where Ω is the set of all elementary events $\omega \in \Omega$, \mathcal{F} is a σ -algebra on Ω and \mathbb{P} is a probability measure. We further consider a second measurable space $(E, \mathcal{B}(E))$, with E being a Banach space and $\mathcal{B}(E)$ the corresponding Borel σ -algebra. An E -valued random field is any mapping $X : \Omega \rightarrow E$ such that $\{\omega \in \Omega : X(\omega) \in B\} \in \mathcal{F}$ holds for any $B \in \mathcal{B}(E)$. For $p \in [1, \infty) \cup \{\infty\}$ we consider the Bochner space $L^p(\Omega; E)$ of p -summable E -valued random variables X equipped with the norm

$$\|X\|_{L^p(\Omega; E)} := \begin{cases} \left(\int_{\Omega} \|X(\omega)\|_E^p d\mathbb{P}(\omega) \right)^{1/p} = \mathbb{E}(\|X\|_E^p)^{1/p}, & 1 \leq p < \infty, \\ \text{esssup}_{\omega \in \Omega} \|X(\omega)\|_E, & p = \infty. \end{cases}$$

In the following we consider absolutely continuous, real-valued random variables $\xi : \Omega \rightarrow \mathbb{R}$; this means that there exists a density function $p_{\xi} : \mathbb{R} \rightarrow \mathbb{R}_+$, such that $\int_{\mathbb{R}} p_{\xi}(y) dy = 1$ and $\mathbb{P}[\xi(\omega) \in A] = \int_A p_{\xi}(y) dy$ for any $A \in \mathcal{B}(\mathbb{R})$. We use the convention that vectors are written using bold fonts.

For $T \in (0, \infty)$ and $f \in C^2(\mathbb{R})$ the equation of interest is the scalar conservation law with uncertain initial data and source term:

$$\begin{aligned} \partial_t u(t, x, \xi(\omega)) + \partial_x f(u(t, x, \xi(\omega))) &= S(t, x, \xi(\omega)), \quad (t, x, \omega) \in (0, T) \times [0, 1]_{\text{per}} \times \Omega, \\ u(0, x, \xi(\omega)) &= u^0(x, \xi(\omega)), \quad (x, \omega) \in [0, 1]_{\text{per}} \times \Omega. \end{aligned} \quad (\text{RIVP})$$

To ensure the existence of weak solutions of (RIVP), via pathwise use of Kružkov's theorem, we impose the following conditions on the initial data and the source term.

- (A1) There exists a constant $M_1 > 0$, such that $\|u^0(\cdot, \xi(\omega))\|_{L^\infty(0,1)} \leq M_1$, \mathbb{P} -a.s. $\omega \in \Omega$ and we have $u^0 \in L^2(\Omega; L^2(0, 1))$.
- (A2) There exists a constant $M_2 > 0$, such that $\|S(\cdot, \cdot, \xi(\omega))\|_{L^\infty((0,T) \times (0,1))} \leq M_2$, \mathbb{P} -a.s. $\omega \in \Omega$ and $S \in L^2(\Omega; L^2((0, T) \times (0, 1))), S(\cdot, \cdot, \xi(\omega)) \in C^1([0, T] \times [0, 1]_{\text{per}})$, \mathbb{P} -a.s. $\omega \in \Omega$.

To ensure uniqueness of a weak solution of (RIVP) we apply the well-known entropy criterion. We say that a convex function $\eta \in C^1(\mathbb{R})$ and $q \in C^1(\mathbb{R})$ form an entropy/entropy-flux pair (η, q) if they satisfy $q' = \eta' f'$. Following the definition in [Mishra & Schwab \(2012\)](#) we define random entropy solutions, which correspond \mathbb{P} -a.s. to entropy solutions as in the deterministic case.

DEFINITION 2.1 (Random entropy solution). We call a weak solution $u \in L^2(\Omega; L^1((0, T) \times (0, 1)))$, with $u(\cdot, \cdot, \xi(\omega)) \in L^\infty((0, T) \times (0, 1))$, \mathbb{P} -a.s. $\omega \in \Omega$, a **random entropy solution** of (RIVP) if the inequality

$$\begin{aligned} &\int_0^T \int_0^1 \eta(u(t, x, \xi(\omega))) \partial_t \phi(t, x) + q(u(t, x, \xi(\omega))) \partial_x \phi(t, x) \, dx \, dt \\ &+ \int_0^T \int_0^1 S(t, x, \xi(\omega)) \eta'(u(t, x, \xi(\omega))) \phi(t, x) \, dx \, dt + \int_0^1 \eta(u^0(x, \xi(\omega))) \phi(0, x) \, dx \geq 0 \end{aligned} \quad (2.1)$$

holds \mathbb{P} -a.s. $\omega \in \Omega$, for all $\phi \in C_c^\infty([0, T] \times [0, 1]_{\text{per}}, \mathbb{R}_+)$ and for all entropy/entropy-flux pairs (η, q) .

REMARK 2.2 For $u(\cdot, \cdot, \xi(\omega)) \in L^\infty((0, T) \times (0, 1))$, \mathbb{P} -a.s. $\omega \in \Omega$ we have

$$\partial_t \eta(u(\cdot, \cdot, \xi(\omega))) + \partial_x q(u(\cdot, \cdot, \xi(\omega))) - S(\cdot, \cdot, \xi(\omega)) \eta'(u(\cdot, \cdot, \xi(\omega))) \leq 0$$

in the distributional sense. Therefore, this distribution has a sign and, thus, is a measure. Then we may replace the smooth test functions in Definition 2.1 by Lipschitz continuous ones; cf. [Dafermos \(2016, Section 4.5\)](#).

In [Mishra & Schwab \(2012\)](#) it is shown that under the conditions (A1) and (A2), there exists a unique random entropy solution $u \in L^2(\Omega; C((0, T); L^1(0, 1)))$ of (RIVP). The approach relies on the pathwise existence and uniqueness of entropy solutions of the scalar conservation law and the following pathwise

mapping properties of the data-to-solution operator $\mathcal{S}(t) : u^0(\cdot, \xi(\omega)) \mapsto \mathcal{S}(t)u^0(\cdot, \xi(\omega))$. These can be found in Kružkov (1970) and will be useful for the proof of Lemma 2.4 below.

- $L^1(0, 1)$ -contraction:

$$\|\mathcal{S}(t)u^0(\cdot, \xi(\omega)) - \mathcal{S}(t)v^0(\cdot, \xi(\omega))\|_{L^1(0,1)} \leq \|u^0(\cdot, \xi(\omega)) - v^0(\cdot, \xi(\omega))\|_{L^1(0,1)}$$

for almost all $t \in (0, T)$, \mathbb{P} -a.s. $\omega \in \Omega$.

- $L^\infty(0, 1)$ -boundedness: there exists a constant $M_3 = M_3(T, M_1, M_2) > 0$ such that

$$\|\mathcal{S}(t)u^0(\cdot, \xi(\omega))\|_{L^\infty(0,1)} \leq M_3$$

for almost all $t \in (0, T)$, \mathbb{P} -a.s. $\omega \in \Omega$.

REMARK 2.3 Although we apply Kružkov's notion of entropy solutions for the well-posedness of (RIVP), our *a posteriori* estimates rely on the relative entropy framework of Dafermos instead of Kružkov's doubling of variables technique. This has three advantages. First, for smooth solutions, upper bounds for the numerical error that result from Kružkov's theory are only of half-order, i.e. have a rate of convergence of $(p + 1)/2$, when $p \in \mathbb{N}$ is the polynomial degree; cf. Gosse & Makridakis (2000) and Kröner & Ohlberger (2000). In contrast, the worst case for error bounds for smooth solutions obtained using the relative entropy framework is losing one order, i.e. the rate of convergence is p . Secondly, the resulting residual of the relative entropy framework allows for an orthogonal decomposition into a spatial (deterministic) residual and a stochastic residual. This decomposition relies on a discretization error estimate for the stochastic Galerkin system and, thus, cannot be obtained when using Kružkov estimates. Finally, the relative entropy framework requires only one strictly convex entropy/entropy flux pair and, hence, is extendible to the systems case.

In the following sections we are dealing with the Bochner space $L^2(\Omega; L^2((0, T) \times (0, 1)))$, instead of $L^2(\Omega; L^1((0, T) \times (0, 1)))$ as in Mishra & Schwab (2012). To ensure that the Bochner integrals are well defined we prove the following.

LEMMA 2.4 Under conditions (A1) and (A2) the mapping

$$(\Omega, \mathcal{F}) \ni \omega \mapsto u(\cdot, \cdot, \xi(\omega)) \in (L^2((0, T) \times (0, 1)), \mathcal{B}(L^2((0, T) \times (0, 1))))$$

is measurable.

Proof. We use the interpolation inequality $\|f\|_{L^2}^2 \leq \|f\|_{L^1} \|f\|_{L^\infty}$ to estimate for almost all $t \in (0, T)$ and $u_0, v_0 \in L^\infty(0, 1)$,

$$\begin{aligned} \|\mathcal{S}(t)u_0 - \mathcal{S}(t)v_0\|_{L^2(0,1)} &\leq \|\mathcal{S}(t)u_0 - \mathcal{S}(t)v_0\|_{L^1(0,1)}^{1/2} \|\mathcal{S}(t)u_0 - \mathcal{S}(t)v_0\|_{L^\infty(0,1)}^{1/2} \\ &\leq (2M_3)^{1/2} \|\mathcal{S}(t)u_0 - \mathcal{S}(t)v_0\|_{L^1(0,1)}^{1/2} \\ &\leq (2M_3)^{1/2} \|u_0 - v_0\|_{L^1(0,1)}^{1/2} \\ &\leq (2M_3)^{1/2} \|u_0 - v_0\|_{L^2(0,1)}^{1/2}. \end{aligned}$$

Therefore, the data-to-solution operator $\mathcal{S}(t) : L^2(0, 1) \rightarrow L^2(0, 1)$ is Hölder continuous with exponent $1/2$ for almost all $t \in (0, T)$. We immediately obtain that the mapping $\mathcal{S} : L^2(0, 1) \ni u_0(\cdot) \mapsto \mathcal{S}(\cdot)u_0(\cdot) \in L^2((0, T) \times (0, 1))$ is also Hölder continuous with exponent $1/2$. Using the fact that the Borel σ -algebra $\mathcal{B}(L^2(0, 1))$ is the smallest σ -algebra containing all open subsets of $L^2(0, 1)$ and that $\mathcal{S}^{-1}(B)$ is open for $B \in \mathcal{B}(L^2((0, T) \times (0, 1)))$, it follows by the continuity of \mathcal{S} , that \mathcal{S} is a measurable mapping from $(L^2(0, 1), \mathcal{B}(L^2(0, 1)))$ to $(L^2((0, T) \times (0, 1)), \mathcal{B}(L^2((0, T) \times (0, 1))))$. For u^0 as in (A1) the map $(\Omega, \mathcal{F}) \ni \omega \mapsto u^0(\cdot, \xi(\omega)) \in (L^2(0, 1), \mathcal{B}(L^2(0, 1)))$ is measurable. Thus, we have that $(\Omega, \mathcal{F}) \ni \omega \mapsto u(\cdot, \cdot, \xi(\omega)) = S(\cdot)u^0(\cdot, \xi(\omega)) \in (L^2((0, T) \times (0, 1)), \mathcal{B}(L^2((0, T) \times (0, 1))))$ is measurable as a composition of measurable functions. \square

Let us now introduce the SG method. We first expand the solution of (RIVP) into a generalized Fourier series using a suitable orthonormal basis. Let $\{\Psi_i(\xi(\cdot))\}_{i \in \mathbb{N}_0} : \Omega \rightarrow \mathbb{R}$ be an $L^2(\Omega)$ -orthonormal basis with respect to the density function p_ξ , i.e. for $i, j \in \mathbb{N}_0$ we have

$$\begin{aligned} \langle \Psi_i, \Psi_j \rangle &:= \mathbb{E}(\Psi_i \Psi_j) = \int_{\Omega} \Psi_i(\xi(\omega)) \Psi_j(\xi(\omega)) \, d\mathbb{P}(\omega) \\ &= \int_{\mathbb{R}} \Psi_i(x) \Psi_j(x) p_\xi(x) \, dx = \delta_{i,j}. \end{aligned} \tag{2.2}$$

Following Wiener (1938) and Abgrall & Mishra (2017), the random entropy solution $u \in L^2(\Omega; L^1((0, T) \times (0, 1)))$ of (RIVP) can be written

$$u(t, x, \xi(\omega)) = \sum_{n=0}^{\infty} u_n(t, x) \Psi_n(\xi(\omega)). \tag{2.3}$$

The deterministic Fourier modes $u_n = u_n(t, x)$ in (2.3) are defined by

$$u_n(t, x) = \mathbb{E}(u(t, x, \xi(\cdot)) \Psi_n(\xi(\cdot))) \quad \forall n \in \mathbb{N}_0.$$

From the Fourier modes we can immediately extract the expectation and variance of u , namely

$$\mathbb{E}(u(t, x, \xi(\omega))) = u_0(t, x) \quad \text{and} \quad \text{Var}(u(t, x, \xi(\omega))) = \sum_{n=1}^{\infty} u_n(t, x)^2.$$

For the error estimates in Section 3 we need an additional assumption on the choice of the orthonormal basis.

ASSUMPTION 2.5 We assume that the elements of the $L^2(\Omega)$ -orthonormal basis $\{\Psi_n(\xi(\cdot))\}_{n=0}^{\infty}$ (w.r.t. the scalar product (2.2)) are essentially bounded in $L^\infty(\Omega)$, i.e. for all $n \in \mathbb{N}_0$ we have

$$\|\Psi_n(\xi(\cdot))\|_{L^\infty(\Omega)} < \infty.$$

Let us mention three examples of orthonormal bases satisfying Assumption 2.5.

EXAMPLE 2.6

1. The classical generalized polynomial chaos approach uses global polynomials that satisfy (2.2) for the corresponding probability density function. In this case one chooses Legendre polynomials if random variables are uniformly distributed, or Jacobi polynomials for a beta distribution. See [Xiu & Karniadakis \(2002\)](#) for more details. For a normal distribution the corresponding Hermite polynomials do not satisfy Assumption 2.5; however, one can scale the Hermite polynomials by $e^{-\xi(\omega)/2}$ to obtain the so-called Hermite functions. Due to the Cramér inequality this orthonormal system is again bounded; cf. [Erdélyi *et al.* \(1981, p. 207\)](#).
2. Instead of choosing a polynomial basis we can choose a discontinuous Haar wavelet basis as in [Le Maître *et al.* \(2004\)](#).
3. Another approach is the multielement approach. For its illustration we assume that $\Omega = [0, 1]$ and decompose Ω into 2^{N_e} , $N_e \in \mathbb{N}_0$ elements:

$$\Omega = \bigcup_{l=0}^{2^{N_e}-1} [2^{-N_e}l, 2^{-N_e}(l+1)].$$

We introduce on each stochastic element $I_l^{N_e} := [2^{-N_e}l, 2^{-N_e}(l+1)]$ the shifted and scaled family of orthonormal polynomials:

$$\Psi_{n,l}^{N_e}(\xi(\omega)) = \begin{cases} 2^{N_e/2}\Psi_n(2^{N_e}\xi(\omega) - l), & \xi(\omega) \in I_l^{N_e}, \\ 0 & \text{otherwise,} \end{cases}$$

for all $n = 0, \dots, N$, $l = 0, \dots, 2^{N_e} - 1$. Here Ψ_n are either the classical orthonormal polynomials from (1), or a wavelet basis as in (2). If we introduce the indices $m = (N+1)l + i$, $i = 0, \dots, N$, $\tilde{N} := (N+1)2^{N_e}$ and define $\Psi_m := \Psi_{n,l}^{N_e}$, $u_m := u_{n,l}^{N_e}$, we may write (cf. [Müller, 2003](#), [Bürger *et al.*, 2014](#) and [Köppel *et al.*, 2017](#))

$$u(t, x, \xi(\omega)) = \lim_{N_e, N \rightarrow \infty} \sum_{m=0}^{\tilde{N}} u_m(t, x) \Psi_m(\xi(\omega)) \quad \text{in } L^2(\Omega).$$

We now truncate the infinite series (2.3) at $N \in \mathbb{N}_0$:

$$\sum_{m=0}^N u_m(t, x) \Psi_m(\xi(\omega)), \quad (t, x, \omega) \in (0, T) \times [0, 1]_{\text{per}} \times \Omega. \quad (2.4)$$

To obtain a weak formulation of (RIVP) on the finite-dimensional space with respect to $\omega \in \Omega$ we insert (2.4) and test the resulting equation against $\{\Psi_i(\xi)\}_{i=0}^N$. Using the orthogonality relation (2.2) yields the

truncated SG system

$$\partial_t u_l(t, x) + \left\langle \partial_x f \left(\sum_{n=0}^N u_n(t, x) \Psi_n(\xi) \right), \Psi_l \right\rangle = \langle S, \Psi_l \rangle \quad \forall l = 0, \dots, N. \quad (\text{S})$$

With a slight abuse of notation we define $\mathbf{u} := (u_0, \dots, u_N)^\top \in \mathbb{R}^{N+1}$, $\mathbf{S} \in \mathbb{R}^{N+1}$, $\mathbf{S}_i := \int_{\Omega} S \Psi_i \, d\mathbb{P}(\omega)$ and $\mathbf{f} : \mathbb{R}^{N+1} \rightarrow \mathbb{R}^{N+1}$, $\mathbf{f}(\mathbf{u})_i := \int_{\Omega} f(\sum_{n=0}^N u_n \Psi_n) \Psi_i \, d\mathbb{P}(\omega)$. We then may write the initial value problem for (S) in the conservation form

$$\begin{aligned} \partial_t \mathbf{u} + \partial_x \mathbf{f}(\mathbf{u}) &= \mathbf{S}, \quad (t, x) \in (0, T) \times [0, 1]_{\text{per}}, \\ \mathbf{u}^0 &= \left(\langle u^0, \Psi_l \rangle \right)_{l=0}^N, \quad x \in [0, 1]_{\text{per}}. \end{aligned} \quad (\text{SG})$$

We give two examples for the structure of the (SG) system, for global orthonormal polynomials.

EXAMPLE 2.7

- (a) We consider the linear advection equation, i.e. $f(u) = au$ for $a \in \mathbb{R}$. In this case system (SG) decouples into $N + 1$ scalar advection equations. This is due to

$$\mathbf{f}(\mathbf{u})_i = a \int_{\Omega} \sum_{n=0}^N u_n \Psi_n \Psi_i \, d\mathbb{P}(\omega) = au_i,$$

and therefore (SG) takes the form

$$\partial_t \mathbf{u} + a \partial_x \mathbf{u} = \mathbf{S}.$$

- (b) For the Burgers equation, i.e. (RIVP) with $f(u) = \frac{u^2}{2}$, we use the symmetric triple product matrices $[C_k]_{i,j=0}^N := \int_{\Omega} \Psi_j \Psi_i \Psi_k \, d\mathbb{P}(\omega)$, which are well defined due to Assumption 2.5. They enable us to rewrite the (SG) system of the Burgers equation as

$$\partial_t \mathbf{u}_k + \frac{1}{2} \partial_x (\mathbf{u}^\top C_k \mathbf{u}) = \mathbf{S}_k$$

for all $k = 0, \dots, N$. Therefore, system (SG) of the Burgers equation is a hyperbolic system but highly coupled; cf. Després *et al.* (2013).

3. Spatio-temporal-stochastic reconstructions and *a posteriori* error analysis

In this section we prove the main theorem of this contribution. We first consider space-time reconstructions for fully discrete DG schemes applied to system (SG). We then introduce space-time stochastic reconstructions to prove an *a posteriori* error estimate for the random scalar conservation law (RIVP), using the relative entropy framework of Dafermos (2016). Finally, we prove the orthogonal decomposition of the space-time stochastic residual into a spatial and a stochastic residual.

3.1 The DG scheme for the SG-system and space-time reconstructions

We briefly recall the DG spatial discretization as for example in Cockburn & Shu (1998, 2001). Let $0 = x_0 < x_1 < \dots < x_M = 1$ be a quasi-uniform triangulation of $[0,1]$ and $0 = t_0 < t_1 < \dots < t_{N_t} = T$ be a temporal decomposition of $[0, T]$. We identify $x_0 = x_M$ to account for the periodic boundary conditions, set $\Delta t_n := (t_{n+1} - t_n)$ for the temporal mesh and $h_k = (x_{k+1} - x_k)$ for the spatial mesh. We now define the (spatial) piecewise polynomial DG spaces for $p \in \mathbb{N}_0$:

$$V_p^s := \{ \mathbf{w} : [x_0, x_M] \rightarrow \mathbb{R}^{N+1} \mid \mathbf{w}|_{(x_{i-1}, x_i)} \in \mathbb{P}_p((x_{i-1}, x_i), \mathbb{R}^{N+1}), 1 \leq i \leq M \}.$$

After spatial discretization of (SG) we obtain the following semidiscrete scheme for the discrete solution $\mathbf{u}_h \in C^1([0, T]; V_p^s)$:

$$\begin{aligned} \sum_{i=0}^{M-1} \int_{x_i}^{x_{i+1}} \partial_t \mathbf{u}_h \cdot \boldsymbol{\psi}_h \, dx &= \sum_{i=0}^{M-1} \int_{x_i}^{x_{i+1}} (\mathbf{f}(\mathbf{u}_h) \cdot \partial_x \boldsymbol{\psi}_h + \mathbf{S} \cdot \boldsymbol{\psi}_h) \, dx - \sum_{i=0}^{M-1} \mathbf{G}(\mathbf{u}_h(x_i^-), \mathbf{u}_h(x_i^+)) \cdot [\![\boldsymbol{\psi}_h]\!]_i, \\ \mathbf{u}_h(t=0) &= \mathcal{I}_{V_p^s} \mathbf{u}_h^0, \end{aligned} \quad (\text{DG-SG})$$

for all $\boldsymbol{\psi}_h \in V_p^s$. Here $\mathcal{I}_{V_p^s}$ is an interpolation or projection operator, $\mathbf{G} : \mathbb{R}^{N+1} \times \mathbb{R}^{N+1} \rightarrow \mathbb{R}^{N+1}$ denotes a numerical flux, the spatial traces are defined as $\boldsymbol{\psi}(x^\pm) := \lim_{h \searrow 0} \boldsymbol{\psi}(x \pm h)$ and $[\![\boldsymbol{\psi}_h]\!]_i := (\boldsymbol{\psi}_h(x_i^-) - \boldsymbol{\psi}_h(x_i^+))$ are jumps. To account for the periodic boundary condition we set $\mathbf{u}_h(x_0^-) = \mathbf{u}_h(x_M^-)$, $\mathbf{u}_h(x_M^+) = \mathbf{u}_h(x_0^+)$. The initial value problem (DG-SG) can now be solved numerically by any single- or multistep method. We focus on \mathcal{K} -order Runge–Kutta time-step methods as in Cockburn & Shu (2001). In writing down the method we denote by $L_h(\mathbf{u}_h(t, \cdot))$ the right-hand side of (DG-SG), with the operator $L_h : V_p^s \rightarrow V_p^s$ being defined appropriately. Furthermore, $\Lambda \Pi_h : \mathbb{R}^{N+1} \rightarrow \mathbb{R}^{N+1}$ is the Total Variation Bounded in the Means (TVBM) minmod slope limiter from Cockburn & Shu (2001). Then the complete S -stage time-marching algorithm for given n th time-iterate $\mathbf{u}_h^n \in V_p^s$ reads as follows:

1. Set $\mathbf{u}_h^{(0)} = \mathbf{u}_h^n$.
2. For $j = 1, \dots, S$ compute the auxiliary functions:

$$\mathbf{u}_h^{(j)} = \Lambda \Pi_h \left(\sum_{l=0}^{j-1} \alpha_{jl} \mathbf{w}_h^{jl} \right), \quad \mathbf{w}_h^{jl} = \mathbf{u}_h^{(l)} + \frac{\beta_{jl}}{\alpha_{jl}} \Delta t_n L_h(\mathbf{u}_h^{(l)}).$$

3. Set $\mathbf{u}_h^{n+1} = \mathbf{u}_h^{(S)}$.

The parameters α_{jl}, β_{jl} satisfy the conditions $\alpha_{jl} \geq 0$, $\sum_{l=0}^{j-1} \alpha_{jl} = 1$, and if $\beta_{jl} \neq 0$, then $\alpha_{jl} \neq 0$ for all $j = 1, \dots, \mathcal{K}, l = 0, \dots, j$.

The relative entropy framework requires one quantity that is at least Lipschitz continuous in space and time. We cannot expect that the entropy solution of (RIVP) satisfies this condition; therefore, we reconstruct the numerical solution of (DG-SG) to obtain a Lipschitz continuous function in space and time. Following Dedner & Giesselmann (2016) we define the **temporal reconstruction** $\hat{\mathbf{u}}^t$ as a C^0 - or even C^1 -function (depending on the polynomial degree) that is piecewise polynomial. From a practical perspective it makes sense to choose the polynomial degree of the reconstruction such that it matches the

formal convergence order of the time-stepping method. This choice ensures that the temporal residual has the same order of convergence as the temporal discretization error (Dedner & Giesselmann, 2016, Theorem 13). Thus, the error estimator enables us to detect whether the convergence order is reduced, e.g. in case f is not sufficiently smooth for the formal convergence order to be reached. Let $\{\mathbf{u}_h^0, \dots, \mathbf{u}_h^{N_t}\}$ be a sequence of approximate solutions of (DG-SG) at points $\{t_n\}_{n=0}^{N_t}$ in time. For the reconstruction in time we define for any vector space V the spaces of piecewise polynomials in time of degree r by

$$V_r^t((0, T); V) := \{\mathbf{w} : [0, T] \rightarrow V \mid \mathbf{w}|_{(t_n, t_{n+1})} \in \mathbb{P}_r((t_n, t_{n+1}), V)\}.$$

Using the methodology proposed in Dedner & Giesselmann (2016), which consists of Hermite interpolations on each time interval $[t_n, t_{n+1}]$, we construct a temporal reconstruction $\hat{\mathbf{u}}^t \in V_r^t((0, T); V_p^s)$. With the temporal reconstruction at hand we now define the space-time reconstruction of the DG solutions of (SG). The analysis in Dedner & Giesselmann (2016) requires numerical fluxes \mathbf{G} that admit a special representation. In particular, there needs to exist a locally Lipschitz function $\mathbf{w} : \mathbb{R}^{N+1} \times \mathbb{R}^{N+1} \rightarrow \mathbb{R}^{N+1}$, with the additional property $\mathbf{w}(\mathbf{u}, \mathbf{u}) = \mathbf{u}$, such that \mathbf{G} can be expressed as

$$\mathbf{G}(\mathbf{u}, \mathbf{v}) = \mathbf{f}(\mathbf{w}(\mathbf{u}, \mathbf{v})) \quad \forall \mathbf{u}, \mathbf{v} \in \mathbb{R}^{N+1}. \quad (3.1)$$

For our numerical computations we consider the upwind flux with $\mathbf{w}(\mathbf{u}, \mathbf{v}) = \mathbf{u}$ and the Lax–Wendroff flux with $\mathbf{w}(\mathbf{u}, \mathbf{v}) = \frac{\mathbf{u} + \mathbf{v}}{2} - \frac{\Delta t}{2h}(\mathbf{f}(\mathbf{u}) - \mathbf{f}(\mathbf{v}))$, both satisfying (3.1) and $\mathbf{w}(\mathbf{u}, \mathbf{u}) = \mathbf{u}$.

We now define the spatial reconstruction that is applied to the temporal reconstruction $\hat{\mathbf{u}}^t(t, \cdot)$ for each $t \in (0, T)$ using the function \mathbf{w} (cf. Giesselmann *et al.*, 2015 and Dedner & Giesselmann, 2016).

DEFINITION 3.1 (Space-time reconstruction). Let $\hat{\mathbf{u}}^t$ be the temporal reconstruction of a sequence $\{\mathbf{u}_h^n\}_{n=0}^{N_t}$ of solutions of the fully discrete scheme of (DG-SG) using a numerical flux satisfying (3.1). The **space-time reconstruction** $\hat{\mathbf{u}}^{\text{st}}(t, \cdot) \in V_{p+1}^s$ is defined as the solution of

$$\begin{aligned} \sum_{i=0}^{M-1} \int_{x_i}^{x_{i+1}} (\hat{\mathbf{u}}^{\text{st}}(t, \cdot) - \hat{\mathbf{u}}^t(t, \cdot)) \cdot \psi \, dx &= 0 \quad \forall \psi \in V_{p-1}^s, \\ \hat{\mathbf{u}}^{\text{st}}(t, x_k^\pm) &= \mathbf{w}(\hat{\mathbf{u}}^t(t, x_k^-), \hat{\mathbf{u}}^t(t, x_k^+)) \quad \forall k = 0, \dots, M. \end{aligned}$$

We have the following property of the space-time reconstruction.

LEMMA 3.2 Let $\hat{\mathbf{u}}^{\text{st}}$ be the space-time reconstruction from Definition 3.1. For each $t \in (0, T)$, the function $\hat{\mathbf{u}}^{\text{st}}(t, \cdot)$ is well defined. Moreover,

$$\hat{\mathbf{u}}^{\text{st}} \in W_\infty^1((0, T); V_{p+1}^s \cap C^0[0, 1]_{\text{per}}).$$

Proof. Cf. Dedner & Giesselmann (2016, Lemma 24). □

Since $\hat{\mathbf{u}}^{\text{st}}$ is Lipschitz continuous in space and time we can compute the space-time residual.

DEFINITION 3.3 (Space-time residual). We define $\mathbf{R}^{\text{st}} := \partial_t \hat{\mathbf{u}}^{\text{st}} + \partial_x \mathbf{f}(\hat{\mathbf{u}}^{\text{st}}) - \mathbf{S} \in L^2((0, T) \times (0, 1); \mathbb{R}^{N+1})$ to be the **space-time residual**.

3.2 Space-time stochastic reconstructions and a posteriori estimate for the random scalar conservation law

Expanding the space-time reconstruction $\hat{\mathbf{u}}^{\text{st}}$ from Section 3.1 in the finite orthonormal system $\{\Psi_i(\xi(\omega))\}_{i=0}^N$ enables us to consider the so-called space-time stochastic residual, which is a crucial part for the upcoming *a posteriori* error estimate. Before defining the space-time stochastic residual we first give a definition of what our approximation of a random entropy solution of (RIVP) is. For simplicity we will write $u(t, x, \omega)$ for $u(t, x, \xi(\omega))$.

DEFINITION 3.4 (Numerical solution of (RIVP)). Let $\{\mathbf{u}_h^0, \dots, \mathbf{u}_h^{N_t}\}$ be the sequence of solutions of (DG-SG) at points $\{t_n\}_{n=0}^{N_t}$ in time. For $n = 0, \dots, N_t$, $u_h^n(x, \omega) = \sum_{i=0}^N (\mathbf{u}_h^n(x))_i \Psi_i(\omega)$ is called the **numerical solution of (RIVP)**.

DEFINITION 3.5 (Space-time stochastic residual). Let $\hat{u}^{\text{sts}}(t, x, \omega) := \sum_{l=0}^N (\hat{\mathbf{u}}^{\text{st}})_l(t, x) \Psi_l(\omega) \in L^2(\Omega) \otimes (W_\infty^1(0, T); (\bar{V}_{p+1}^s \cap C^0([0, 1]_{\text{per}})))$ be the **space-time–stochastic reconstruction**, where

$$\bar{V}_p^s := \{w : [x_0, x_M] \rightarrow \mathbb{R} \mid w|_{(x_{i-1}, x_i)} \in \mathbb{P}_p((x_{i-1}, x_i), \mathbb{R}), 1 \leq i \leq M\}.$$

We define the **space-time stochastic residual** by

$$\mathcal{R}^{\text{sts}} := \partial_t \hat{u}^{\text{sts}} + \partial_x f(\hat{u}^{\text{sts}}) - S \in L^2((0, T) \times (0, 1) \times \Omega; \mathbb{R}). \quad (3.2)$$

For the proof of the main theorem of this article we need the notion of the relative entropy and the relative entropy flux. We follow the definition in Dafermos (2016, Section 5.2).

DEFINITION 3.6 (Relative entropy and entropy flux). We define the **relative entropy** $\eta(\cdot|\cdot) : \mathbb{R} \times \mathbb{R} \rightarrow \mathbb{R}$ and the **relative entropy flux** $q(\cdot|\cdot) : \mathbb{R} \times \mathbb{R} \rightarrow \mathbb{R}$ by

$$\eta(u|v) = \eta(u) - \eta(v) - \eta'(v)(u - v), \quad (3.3)$$

$$q(u|v) = q(u) - q(v) - \eta'(v)(f(u) - f(v)). \quad (3.4)$$

EXAMPLE 3.7 (Relative entropy). For $\eta(u) = \frac{u^2}{2}$ we compute

$$\eta(u|v) = \frac{u^2 - v^2}{2} - v(u - v) = \frac{(u - v)^2}{2}. \quad (3.5)$$

This choice is used in the proof of Theorem 3.8 below. For arbitrary strictly convex $\eta \in C^2(\mathbb{R})$, an analogous proof leads to very similar estimates that contain constants related to the modulus of convexity of η ; see Dedner & Giesselmann (2016) for further details.

Using the relative entropy framework we are able to derive the following *a posteriori* error bound for (RIVP).

THEOREM 3.8 (*A posteriori* error bound for the reconstruction of the numerical solution). Let u be a random entropy solution of (RIVP). Then the difference between u and the reconstruction \hat{u}^{sts} from

Definition 3.5 satisfies

$$\|u(s, \cdot, \cdot) - \hat{u}^{\text{sts}}(s, \cdot, \cdot)\|_{L^2((0,1) \times \tilde{\Omega})}^2 \leq \left(\mathcal{E}^{\text{sts}}(s) + \mathcal{E}_0^{\text{sts}} \right) \exp \left(\int_0^s \left(C_{f''} \|\partial_x \hat{u}^{\text{sts}}(t, \cdot, \cdot)\|_{L^\infty((0,1) \times \tilde{\Omega})} + \frac{1}{4} \right) dt \right)$$

for $0 \leq s \leq T$ and for any \mathbb{P} -measurable set $\tilde{\Omega} \subset \Omega$. Here

$$\mathcal{E}^{\text{sts}}(t) := \|\mathcal{R}^{\text{sts}}\|_{L^2((0,t) \times (0,1) \times \tilde{\Omega})}^2, \quad (3.6)$$

$$\mathcal{E}_0^{\text{sts}} := \|u^0 - \hat{u}^{\text{sts}}(0, \cdot, \cdot)\|_{L^2((0,1) \times \tilde{\Omega})}^2 \quad (3.7)$$

and $C_{f''} := \max_{u \in M} \frac{|f''(u)|}{2}$, with $M := \text{Conv}([-M_3, M_3] \cup \text{Ran}(\hat{u}^{\text{sts}}))$, where Conv denotes the convex hull and Ran the image of \hat{u}^{sts} .

By means of the triangle inequality we can formulate Theorem 3.8 in terms of the numerical solution u_h^n of (RIVP).

COROLLARY 3.9 (*A posteriori* error bound for the numerical solution). Let u be a random entropy solution of (RIVP). Then the difference between u and the numerical solution u_h^n from Definition 3.4 satisfies

$$\begin{aligned} \|u(t_n, \cdot, \cdot) - u_h^n(\cdot, \cdot)\|_{L^2((0,1) \times \tilde{\Omega})}^2 &\leq 2\|\hat{u}^{\text{sts}}(t_n, \cdot, \cdot) - u_h^n(\cdot, \cdot)\|_{L^2((0,1) \times \tilde{\Omega})}^2 \\ &\quad + 2\left(\mathcal{E}^{\text{sts}}(t_n) + \mathcal{E}_0^{\text{sts}}\right) \exp \left(\int_0^{t_n} \left(C_{f''} \|\partial_x \hat{u}^{\text{sts}}(t, \cdot, \cdot)\|_{L^\infty((0,1) \times \tilde{\Omega})} + \frac{1}{4} \right) dt \right) \end{aligned}$$

for all $n = 0, \dots, N_t$ and for all measurable sets $\tilde{\Omega} \subset \Omega$.

REMARK 3.10

1. All quantities in the upper bound of Theorem 3.8 and Corollary 3.9 are computable within a numerical simulation. However, the computation of the image of \hat{u}^{sts} , $\text{Ran}(\hat{u}^{\text{sts}})$, can be very expensive, in particular for large DG polynomial degrees.
2. Due to Lemma 3.2 every component of the space-time reconstruction $\hat{\mathbf{u}}^{\text{st}}$ is Lipschitz continuous in space and therefore has a bounded derivative. Combined with Assumption 2.5 we obtain that every summand of

$$\partial_x \hat{u}^{\text{sts}}(t, x, \omega) = \sum_{l=0}^N \partial_x (\hat{\mathbf{u}}^{\text{st}})_l(t, x) \Psi_l(\omega)$$

is in $L^\infty((0, 1) \times \Omega)$, which ensures that the space-time stochastic reconstruction \hat{u}^{sts} satisfies

$$\|\partial_x \hat{u}^{\text{sts}}(s, \cdot, \cdot)\|_{L^\infty((0,1) \times \Omega)} < \infty \quad \forall s \in (0, T].$$

Note that we actually could remove Assumption 2.5 and formulate Theorem 3.8 only for those subsets $\tilde{\Omega} \subset \Omega$ for which $\|\Psi_n(\xi(\cdot))\|_{L^\infty(\tilde{\Omega})} < \infty$ for all $n \in \mathbb{N}_0$.

3. As described in Pettersson *et al.* (2015), the solution of system (SG) may exhibit discontinuities in the spatial variables, even if the solution of the original problem is smooth. In the case that the exact solution of the (SG)-system is discontinuous, the quantity $\|\partial_x \hat{u}^{\text{sts}}\|_{L^\infty(\Omega \times [0,1])}$ is expected to scale like h^{-1} and hence the estimator will blow up for $h \rightarrow 0$ in the vicinity of discontinuities.
4. For linear equations $f(u) = au$, $a \in \mathbb{R}$ we have $C_{f''} = 0$. Therefore, for linear equations we expect no blow-up of the estimator for $h \rightarrow 0$ even in the case that the solution is discontinuous.

REMARK 3.11 (Localization of the error estimators). Due to the pointwise definition of the random entropy solution, the choice of $\tilde{\Omega}$ is arbitrary. This enables us to localize the error estimator in the stochastic variable. With some more effort it is also possible to localize the error estimator in the physical space in a wave cone around the region of interest; cf. the proof of Dafermos (2016, Theorem 5.2.1). For scalar problems and an L^1 -theory, a restriction to a smaller wave cone is possible; see Gosse & Makridakis (2000). The L^2 -theory as in our case is more challenging for the scalar case and, as already noted in Remark 3.10.3, the estimator will blow up in the vicinity of a discontinuity. However, in contrast to the Kružkov framework, the relative entropy framework is extendable to systems of conservation laws and allows us to derive similar error estimators for the case of systems.

Proof of Theorem 3.8. Because u is a pointwise entropy solution of (RIVP) \mathbb{P} -a.s. $\omega \in \Omega$ we can integrate the entropy inequality (2.1) with respect to any \mathbb{P} -measurable $\tilde{\Omega} \subset \Omega$. Thus, we have for any non-negative Lipschitz continuous test function $\phi = \phi(t, x)$ the inequality

$$\begin{aligned} 0 \leq & \int_{\tilde{\Omega}} \int_0^T \int_0^1 \eta(u) \partial_t \phi + q(u) \partial_x \phi \, dx \, dt \, d\mathbb{P}(\omega) + \int_{\tilde{\Omega}} \int_0^T \int_0^1 S \eta'(u) \phi \, dx \, dt \, d\mathbb{P}(\omega) \\ & + \int_{\tilde{\Omega}} \int_0^1 \eta(u^0) \phi(0, x) \, dx \, d\mathbb{P}(\omega). \end{aligned} \quad (3.8)$$

Next we multiply (3.2) by $\eta'(\hat{u}^{\text{sts}})$. Upon using the chain rule for Lipschitz continuous functions and the relationship $q' = \eta' f'$ we derive the following relation:

$$\eta'(\hat{u}^{\text{sts}}) \mathcal{R}^{\text{sts}} = \partial_t(\eta(\hat{u}^{\text{sts}})) + \partial_x q(\hat{u}^{\text{sts}}) - \eta'(\hat{u}^{\text{sts}}) S. \quad (3.9)$$

For the rest of the proof we choose a quadratic entropy function, i.e. we set $\eta(u) = \frac{u^2}{2}$. We then consider the weak form of (3.9), integrate with respect to $\tilde{\Omega} \subset \Omega$ and subtract this from (3.8) to obtain

$$\begin{aligned} 0 \leq & \int_{\tilde{\Omega}} \int_0^T \int_0^1 (\eta(u) - \eta(\hat{u}^{\text{sts}})) \partial_t \phi + (q(u) - q(\hat{u}^{\text{sts}})) \partial_x \phi \, dx \, dt \, d\mathbb{P}(\omega) \\ & - \int_{\tilde{\Omega}} \int_0^T \int_0^1 \mathcal{R}^{\text{sts}} \hat{u}^{\text{sts}} \phi \, dx \, dt \, d\mathbb{P}(\omega) + \int_{\tilde{\Omega}} \int_0^T \int_0^1 S(u - \hat{u}^{\text{sts}}) \phi \, dx \, dt \, d\mathbb{P}(\omega) \\ & + \int_{\tilde{\Omega}} \int_0^1 (\eta(u^0) - \eta(\hat{u}_0^{\text{sts}})) \phi(0, x) \, dx \, d\mathbb{P}(\omega), \end{aligned}$$

with $\hat{u}_0^{\text{sts}} := \hat{u}^{\text{sts}}(0, \cdot, \cdot)$. Using Definition 3.6 of the relative entropy and the relative entropy flux we may write

$$\begin{aligned} 0 \leq & \int_{\tilde{\Omega}} \int_0^T \int_0^1 (\eta(u|\hat{u}^{\text{sts}}) + \hat{u}^{\text{sts}}(u - \hat{u}^{\text{sts}})) \partial_t \phi \, dx \, dt \, d\mathbb{P}(\omega) \\ & + \int_{\tilde{\Omega}} \int_0^T \int_0^1 (q(u|\hat{u}^{\text{sts}}) + \hat{u}^{\text{sts}}(f(u) - f(\hat{u}^{\text{sts}}))) \partial_x \phi \, dx \, dt \, d\mathbb{P}(\omega) \\ & - \int_{\tilde{\Omega}} \int_0^T \int_0^1 \mathcal{R}^{\text{sts}} \hat{u}^{\text{sts}} \phi \, dx \, dt \, d\mathbb{P}(\omega) + \int_{\tilde{\Omega}} \int_0^T \int_0^1 S(u - \hat{u}^{\text{sts}}) \phi \, dx \, dt \, d\mathbb{P}(\omega) \\ & + \int_{\tilde{\Omega}} \int_0^1 (\eta(u^0) - \eta(\hat{u}_0^{\text{sts}})) \phi(0, x) \, dx \, d\mathbb{P}(\omega). \end{aligned} \quad (3.10)$$

Using the Lipschitz continuous (in space and time) test function $\phi \hat{u}^{\text{sts}}$ in the weak form of (RIVP) and in (3.2) we obtain

$$\begin{aligned} 0 = & \int_{\tilde{\Omega}} \int_0^T \int_0^1 (u - \hat{u}^{\text{sts}}) \partial_t (\hat{u}^{\text{sts}} \phi) + (f(u) - f(\hat{u}^{\text{sts}})) \partial_x (\hat{u}^{\text{sts}} \phi) \, dx \, dt \, d\mathbb{P}(\omega) \\ & - \int_{\tilde{\Omega}} \int_0^T \int_0^1 \mathcal{R}^{\text{sts}} \hat{u}^{\text{sts}} \phi \, dx \, dt \, d\mathbb{P}(\omega) + \int_{\tilde{\Omega}} \int_0^1 (u^0 - \hat{u}_0^{\text{sts}}) \phi(0, x) \hat{u}_0^{\text{sts}} \, dx \, d\mathbb{P}(\omega). \end{aligned} \quad (3.11)$$

Using the product rule,

$$\begin{aligned} \partial_t (\hat{u}^{\text{sts}} \phi) &= \partial_t \hat{u}^{\text{sts}} \phi + \partial_t \phi \hat{u}^{\text{sts}}, \\ \partial_x (\hat{u}^{\text{sts}} \phi) &= \partial_x \hat{u}^{\text{sts}} \phi + \partial_x \phi \hat{u}^{\text{sts}}. \end{aligned}$$

Combining (3.11) with (3.10) we obtain

$$\begin{aligned} 0 \leq & \int_{\tilde{\Omega}} \int_0^T \int_0^1 \eta(u|\hat{u}^{\text{sts}}) \partial_t \phi + q(u|\hat{u}^{\text{sts}}) \partial_x \phi - \partial_t \hat{u}^{\text{sts}}(u - \hat{u}^{\text{sts}}) \phi \, dx \, dt \, d\mathbb{P}(\omega) \\ & - \int_{\tilde{\Omega}} \int_0^T \int_0^1 (\partial_x \hat{u}^{\text{sts}}(f(u) - f(\hat{u}^{\text{sts}})) \phi - S(u - \hat{u}^{\text{sts}}) \phi) \, dx \, dt \, d\mathbb{P}(\omega) \\ & + \int_{\tilde{\Omega}} \int_0^1 \eta(u^0|\hat{u}_0^{\text{sts}}) \phi(0, x) \, dx \, d\mathbb{P}(\omega). \end{aligned}$$

Using the fact that

$$\partial_t \hat{u}^{\text{sts}} = -f'(\hat{u}^{\text{sts}}) \partial_x \hat{u}^{\text{sts}} + \mathcal{R}^{\text{sts}} + S$$

we conclude that

$$\begin{aligned}
0 \leq & \int_{\tilde{\Omega}} \int_0^T \int_0^1 \eta(u|\hat{u}^{\text{sts}}) \partial_t \phi + q(u|\hat{u}^{\text{sts}}) \partial_x \phi \, dx \, dt \, d\mathbb{P}(\omega) \\
& - \int_{\tilde{\Omega}} \int_0^T \int_0^1 [-f'(\hat{u}^{\text{sts}}) \partial_x \hat{u}^{\text{sts}} + \mathcal{R}^{\text{sts}} + S](u - \hat{u}^{\text{sts}}) \phi \, dx \, dt \, d\mathbb{P}(\omega) \\
& - \int_{\tilde{\Omega}} \int_0^T \int_0^1 [\partial_x \hat{u}^{\text{sts}} (f(u) - f(\hat{u}^{\text{sts}})) \phi - S(u - \hat{u}^{\text{sts}}) \phi] \, dx \, dt \, d\mathbb{P}(\omega) \\
& + \int_{\tilde{\Omega}} \int_0^1 \eta(u^0|\hat{u}_0^{\text{sts}}) \phi(0, x) \, dx \, d\mathbb{P}(\omega).
\end{aligned}$$

The last inequality is reformulated as

$$\begin{aligned}
0 \leq & \int_{\tilde{\Omega}} \int_0^T \int_0^1 \eta(u|\hat{u}^{\text{sts}}) \partial_t \phi + q(u|\hat{u}^{\text{sts}}) \partial_x \phi \, dx \, dt \, d\mathbb{P}(\omega) \\
& - \int_{\tilde{\Omega}} \int_0^T \int_0^1 \partial_x \hat{u}^{\text{sts}} (f(u) - f(\hat{u}^{\text{sts}}) - f'(\hat{u}^{\text{sts}})(u - \hat{u}^{\text{sts}})) \phi \, dx \, dt \, d\mathbb{P}(\omega) \\
& - \int_{\tilde{\Omega}} \int_0^T \int_0^1 \mathcal{R}^{\text{sts}}(u - \hat{u}^{\text{sts}}) \phi \, dx \, dt \, d\mathbb{P}(\omega) + \int_{\tilde{\Omega}} \int_0^1 \eta(u^0|\hat{u}_0^{\text{sts}}) \phi(0, x) \, dx \, d\mathbb{P}(\omega). \quad (3.12)
\end{aligned}$$

Up to now the choice of ϕ has been arbitrary. Now we fix $s > 0$ and $\epsilon > 0$ and define ϕ as

$$\phi(\sigma, x) := \begin{cases} 1 & : \sigma < s, \\ 1 - \frac{\sigma-s}{\epsilon} & : s < \sigma < s + \epsilon, \\ 0 & : \sigma > s + \epsilon. \end{cases}$$

With this particular choice we obtain

$$\begin{aligned}
0 \leq & -\frac{1}{\epsilon} \int_{\tilde{\Omega}} \int_s^{s+\epsilon} \int_0^1 \eta(u|\hat{u}^{\text{sts}}) \, dx \, dt \, d\mathbb{P}(\omega) \\
& - \int_{\tilde{\Omega}} \int_0^T \int_0^1 \partial_x \hat{u}^{\text{sts}} (f(u) - f(\hat{u}^{\text{sts}}) - f'(\hat{u}^{\text{sts}})(u - \hat{u}^{\text{sts}})) \phi \, dx \, dt \, d\mathbb{P}(\omega) \\
& - \int_{\tilde{\Omega}} \int_0^T \int_0^1 \mathcal{R}^{\text{sts}}(u - \hat{u}^{\text{sts}}) \phi \, dx \, dt \, d\mathbb{P}(\omega) + \int_{\tilde{\Omega}} \int_0^1 \eta(u^0|\hat{u}_0^{\text{sts}}) \, dx \, d\mathbb{P}(\omega).
\end{aligned}$$

Sending $\epsilon \rightarrow 0$ we find for all Lebesgue points s of $\eta(u(\sigma, \cdot, \cdot))$ in $(0, T)$ that

$$\begin{aligned} 0 &\leq - \int_{\tilde{\Omega}} \int_0^1 \eta(u(s, \cdot, \cdot) | \hat{u}^{\text{sts}}(s, \cdot, \cdot)) \, dx \, d\mathbb{P}(\omega) \\ &\quad - \int_{\tilde{\Omega}} \int_0^s \int_0^1 \partial_x \hat{u}^{\text{sts}}(f(u) - f(\hat{u}^{\text{sts}}) - f'(\hat{u}^{\text{sts}})(u - \hat{u}^{\text{sts}})) \, dx \, dt \, d\mathbb{P}(\omega) \\ &\quad - \int_{\tilde{\Omega}} \int_0^s \int_0^1 \mathcal{R}^{\text{sts}}(u - \hat{u}^{\text{sts}}) \, dx \, dt \, d\mathbb{P}(\omega) + \int_{\tilde{\Omega}} \int_0^1 \eta(u^0 | \hat{u}_0^{\text{sts}}) \, dx \, d\mathbb{P}(\omega). \end{aligned}$$

We then estimate

$$\int_{\tilde{\Omega}} \int_0^s \int_0^1 \mathcal{R}^{\text{sts}}(u - \hat{u}^{\text{sts}}) \, dx \, dt \, d\mathbb{P}(\omega)$$

by Young's inequality. The integral

$$\int_{\tilde{\Omega}} \int_0^s \int_0^1 \partial_x \hat{u}^{\text{sts}}(f(u) - f(\hat{u}^{\text{sts}}) - f'(\hat{u}^{\text{sts}})(u - \hat{u}^{\text{sts}})) \, dx \, dt \, d\mathbb{P}(\omega)$$

is estimated by Taylor's theorem which yields the constant $C_{f''}$. The remaining terms are estimated using the explicit form of $\eta(\cdot, \cdot)$, cf. Example 3.7. Altogether we obtain

$$\begin{aligned} &\int_{\tilde{\Omega}} \int_0^1 |u(s, \cdot, \cdot) - \hat{u}^{\text{sts}}(s, \cdot, \cdot)|^2 \, dx \, d\mathbb{P}(\omega) \\ &\leq C_{f''} \int_0^s \left(\|\partial_x \hat{u}^{\text{sts}}(t, \cdot, \cdot)\|_{L^\infty((0,1) \times \tilde{\Omega})} \int_{\tilde{\Omega}} \int_0^1 |u - \hat{u}^{\text{sts}}|^2 \, dx \, d\mathbb{P}(\omega) \right) dt \\ &\quad + \|\mathcal{R}^{\text{sts}}\|_{L^2((0,s) \times (0,1) \times \tilde{\Omega})}^2 + \frac{1}{4} \int_{\tilde{\Omega}} \int_0^s \int_0^1 |u - \hat{u}^{\text{sts}}|^2 \, dx \, dt \, d\mathbb{P}(\omega) \\ &\quad + \|u^0 - \hat{u}^{\text{sts}}(0, \cdot, \cdot)\|_{L^2((0,1) \times \tilde{\Omega})}^2. \end{aligned}$$

Grönwall's inequality yields the assertion. \square

3.3 An orthogonal decomposition of the space-time stochastic residual

Due to Corollary 3.9 we have a computable upper bound for the space-stochastic error between the random entropy solution and its numerical approximation. However, we still cannot distinguish between the errors arising from spatial and stochastic discretization. We therefore want to show a remarkable property of the space-time stochastic residual \mathcal{R}^{sts} from Definition 3.5, which indeed allows us to distinguish between spatial and stochastic error.

To this end we consider the projection of the space-time stochastic residual \mathcal{R}^{sts} onto $\text{span}\{\Psi_0, \dots, \Psi_N\}$ and show that $\langle \mathcal{R}^{\text{sts}}, \Psi_l \rangle$ coincides with the coefficients of the space-time residual \mathbf{R}^{st}

from Definition 3.3. This can be seen from the following computation. Let $l = 0, \dots, N$:

$$\begin{aligned} \langle \mathcal{R}^{\text{sts}}, \Psi_l \rangle &= \left\langle \partial_t \hat{u}^{\text{sts}} + \partial_x f(\hat{u}^{\text{sts}}) - S, \Psi_l \right\rangle = \int_{\Omega} \left(\partial_t \sum_{k=0}^N (\hat{\mathbf{u}}^{\text{st}})_k \Psi_k + \partial_x f \left(\sum_{k=0}^N (\hat{\mathbf{u}}^{\text{st}})_k \Psi_k \right) - S \right) \Psi_l \, d\mathbb{P}(\omega) \\ &= \partial_t (\hat{\mathbf{u}}^{\text{st}})_l + (\partial_x \mathbf{f}(\hat{\mathbf{u}}^{\text{st}}))_l - S_l = (\mathbf{R}^{\text{st}})_l. \end{aligned}$$

Hence, the coefficients of \mathcal{R}^{sts} in the basis $\{\Psi_0, \dots, \Psi_N\}$ are the coefficients of \mathbf{R}^{st} from Definition 3.3 and thus these coefficients are associated with the space-time error that arises when approximating the truncated (deterministic) (SG)-system.

For the remaining coefficients of \mathcal{R}^{sts} there is no such interpretation. But since the (SG)-system is obtained by an orthogonal projection onto $\text{span}\{\Psi_0, \dots, \Psi_N\}$ the remaining coefficients of \mathcal{R}^{sts} contribute the stochastic error that arises when truncating the infinite Fourier series (2.3). This motivates us to gather the higher modes into a vector $\mathbf{R}^{\text{stoch}}$, which we will call the **stochastic residual**. It has for $l > N$ the entries

$$(\mathbf{R}^{\text{stoch}})_l := \langle \mathcal{R}^{\text{sts}}, \Psi_l \rangle = \left\langle \partial_t \hat{u}^{\text{sts}} + \partial_x f(\hat{u}^{\text{sts}}) - S, \Psi_l \right\rangle = \int_{\Omega} \left(\partial_x f \left(\sum_{k=0}^N (\hat{\mathbf{u}}^{\text{st}})_k \Psi_k \right) - S \right) \Psi_l \, d\mathbb{P}(\omega). \quad (3.13)$$

Here we used the orthogonality relation $\langle \partial_t \hat{u}^{\text{sts}}, \Psi_l \rangle = \langle \partial_t \sum_{k=0}^N (\hat{\mathbf{u}}^{\text{st}})_k \Psi_k, \Psi_l \rangle = 0$, which holds for $l > N$. These properties of \mathcal{R}^{sts} translate into the following.

THEOREM 3.12 (Orthogonal decomposition of the space-time stochastic residual). The space-time stochastic residual \mathcal{R}^{sts} , from Definition 3.5, admits the following orthogonal decomposition in $L^2(\Omega)$:

$$\mathcal{R}^{\text{sts}} = \sum_{i=0}^N (\mathbf{R}^{\text{st}})_i \Psi_i + \sum_{i=N+1}^{\infty} (\mathbf{R}^{\text{stoch}})_i \Psi_i. \quad (3.14)$$

Further, $\mathcal{E}^{\text{sts}}(s)$ from (3.6) admits the following decomposition:

$$\mathcal{E}^{\text{sts}}(s) = \mathcal{E}^{\text{st}}(s) + \mathcal{E}^{\text{stoch}}(s), \quad (3.15)$$

where $\mathcal{E}^{\text{st}}(s) := \sum_{i=0}^N \|(\mathbf{R}^{\text{st}})_i\|_{L^2((0,s) \times (0,1))}^2$ and $\mathcal{E}^{\text{stoch}}(s) := \sum_{i=N+1}^{\infty} \|(\mathbf{R}^{\text{stoch}})_i\|_{L^2((0,s) \times (0,1))}^2$ for all $s \in (0, T]$.

Proof. Formula (3.14) follows from the previous computations. Formula (3.15) is an application of the Pythagorean theorem for the Hilbert space $L^2(\Omega)$ applied to $\mathcal{E}^{\text{sts}}(s) = \|\mathcal{R}^{\text{sts}}\|_{L^2((0,s) \times (0,1) \times \Omega)}^2$. \square

REMARK 3.13 In the same manner as for Theorem 3.12 we can find an orthogonal decomposition of the approximation error in the initial condition measured by $\mathcal{E}_0^{\text{sts}}$ given in (3.7). Let us define the orthogonal

projection $\Pi_N(u^0) := \sum_{m=0}^N \langle u^0, \Psi_m \rangle \Psi_m$. Then, the Pythagorean theorem implies

$$\begin{aligned} \mathcal{E}_0^{\text{sts}} &= \|u^0 - \hat{u}^{\text{sts}}(0, \cdot, \cdot)\|_{L^2((0,1) \times \Omega)}^2 = \|u^0 - \Pi_N(u^0)\|_{L^2((0,1) \times \Omega)}^2 + \|\Pi_N(u^0) - \hat{u}^{\text{sts}}(0, \cdot, \cdot)\|_{L^2((0,1) \times \Omega)}^2 \\ &= \left\| \sum_{m=N+1}^{\infty} \langle u^0, \Psi_m \rangle \right\|_{L^2(0,1)}^2 + \sum_{m=0}^N \|\langle u^0, \Psi_m \rangle - \hat{\mathbf{u}}_m^{\text{st}}(0, \cdot)\|_{L^2(0,1)}^2 \\ &=: \mathcal{E}_0^{\text{stoch}} + \mathcal{E}_0^{\text{st}}. \end{aligned} \quad (3.16)$$

We can now combine Corollary 3.9, Theorem 3.12 and Remark 3.13 to obtain an *a posteriori* error bound for the error between the random entropy solution and its numerical approximation, which provides separate bounds for the spatial discretization error and the stochastic discretization error

THEOREM 3.14 (*A posteriori* error bound for the numerical solution with error splitting). Let u be a random entropy solution of (RIVP). Then the difference between u and the numerical solution u_h^n from Definition 3.4 satisfies

$$\begin{aligned} \|u(t_n, \cdot, \cdot) - u_h^n(\cdot, \cdot)\|_{L^2((0,1) \times \tilde{\Omega})}^2 &\leq 2\|\hat{u}^{\text{sts}}(t_n, \cdot, \cdot) - u_h^n(\cdot, \cdot)\|_{L^2((0,1) \times \tilde{\Omega})}^2 \\ &\quad + 2\left(\mathcal{E}^{\text{st}}(t_n) + \mathcal{E}^{\text{stoch}}(t_n) + \mathcal{E}_0^{\text{st}} + \mathcal{E}_0^{\text{stoch}}\right) \\ &\quad \times \exp\left(\int_0^{t_n} \left(C_{f''} \|\partial_x \hat{u}^{\text{sts}}(t, \cdot, \cdot)\|_{L^\infty((0,1) \times \tilde{\Omega})} + \frac{1}{4}\right) dt\right) \end{aligned}$$

for all $n = 0, \dots, N_t$ and for all measurable sets $\tilde{\Omega} \subset \Omega$.

Theorem 3.14 allows us to decompose the error estimator for the space-time stochastic error into parts quantifying the stochastic and the space-time discretization error, respectively. The stochastic error, introduced by truncating the Fourier series in (2.3), can be quantified by $\mathcal{E}^{\text{stoch}}(t_n) + \mathcal{E}_0^{\text{stoch}}$. The space-time discretization error, i.e. the error that arises by discretizing the system (SG) in space and time, can be quantified by $\mathcal{E}^{\text{st}}(t_n) + \mathcal{E}_0^{\text{st}}$. The optimality of \mathcal{E}^{st} in the case of linear hyperbolic equations was proven in Dedner & Giesselmann (2016). Optimality means that the space-time residual has the same order of convergence as the DG scheme. However, in the nonlinear case the optimality of the residual in the first time step is still open. We address this issue in Section 4. For the stochastic residual we expect, at least for smooth solutions, spectral convergence.

We finally want to mention how to compute the entries of the stochastic residual $\mathbf{R}^{\text{stoch}}$ from (3.13) in the case of the linear advection equation and the Burgers equation.

EXAMPLE 3.15

(a) In the case of the linear advection equation $f(u) = au$, $a \in \mathbb{R}$, we have

$$(\mathbf{R}^{\text{stoch}})_l = \int_{\Omega} \left(\partial_x f \left(\sum_{k=0}^N (\hat{\mathbf{u}}^{\text{st}})_k \Psi_k \right) \right) \Psi_l d\mathbb{P}(\omega) = a \sum_{k=0}^N \partial_x (\hat{\mathbf{u}}^{\text{st}})_k \int_{\Omega} \Psi_k \Psi_l d\mathbb{P}(\omega) = 0$$

for $l > N$, due to orthogonality. Thus $\mathbf{R}^{\text{stoch}}$ and consequently $\mathcal{E}^{\text{stoch}}$ vanish. This means that the stochastic error is only inferred from projecting the initial condition onto the orthonormal system,

cf. Example 2.7(a), and can be measured by $\mathcal{E}_0^{\text{stoch}}$. Due to linearity of the advection equation the initial stochastic error does not increase when advancing in time.

- (b) In the case of the Burgers equation $f(u) = \frac{u^2}{2}$ and classical global orthonormal chaos polynomials we get an explicit formula for the entries of the stochastic residual $\mathbf{R}^{\text{stoch}}$, namely for $l > N$,

$$(\mathbf{R}^{\text{stoch}})_l = \int_{\Omega} \left(\partial_x f \left(\sum_{k=0}^N (\hat{\mathbf{u}}^{\text{st}})_k \Psi_k \right) \right) \Psi_l \, d\mathbb{P}(\omega) = \frac{1}{2} \int_{\Omega} \partial_x \left(\sum_{k=0}^N (\hat{\mathbf{u}}^{\text{st}})_k \Psi_k \right)^2 \Psi_l \, d\mathbb{P}(\omega).$$

Because $\left(\sum_{k=0}^N (\hat{\mathbf{u}}^{\text{st}})_k \Psi_k \right)^2$ is a polynomial of degree $2N$ and due to orthogonality, it follows that

$$\int_{\Omega} \partial_x f \left(\sum_{k=0}^N (\hat{\mathbf{u}}^{\text{st}})_k \Psi_k \right) \Psi_l \, d\mathbb{P}(\omega) = 0$$

for $l > 2N$. We therefore need to compute $(\mathbf{R}^{\text{stoch}})_l$ only for $l = N+1, \dots, 2N$. Moreover,

$$\frac{1}{2} \int_{\Omega} \partial_x \left(\sum_{k=0}^N (\hat{\mathbf{u}}^{\text{st}})_k \Psi_k \right)^2 \Psi_l \, d\mathbb{P}(\omega) = (\partial_x \hat{\mathbf{u}}^{\text{st}})^\top C_l \hat{\mathbf{u}}^{\text{st}},$$

where $[C_k]_{i,j=0}^N := \int_{\Omega} \Psi_j \Psi_i \Psi_k \, d\mathbb{P}(\omega)$, $k = N+1, \dots, 2N$ is the symmetric triple product matrix.

- (c) For a multielement approach, as discussed in Remark 2.3 we can compute the spatial and stochastic residuals on each stochastic element $I_l^{N_e}$, $l = 0, \dots, 2N_e$ in parallel.

4. Numerical examples

In this section we present numerical experiments, where we examine the scaling behavior of the space-time–stochastic residual. For the following test cases we consider the classical polynomial chaos expansion using Legendre orthonormal polynomials for uniformly distributed random variables. As the numerical solver for the SG system we use the Runge–Kutta DG solver *Flexi* (Hindenlang *et al.*, 2012). For the time stepping we use an explicit RK3-7 method (Toulorge & Desmet, 2012), a time reconstruction of order 3 and for the physical space we use DG polynomials of degree 1 or 2. As numerical flux for the linear advection equation we choose the upwind flux,

$$\mathbf{G}(\mathbf{u}, \mathbf{v}) = \mathbf{f}(\mathbf{w}(\mathbf{u}, \mathbf{v})), \quad \mathbf{w}(\mathbf{u}, \mathbf{v}) = \mathbf{u},$$

and as projection operator for the initial data we choose the Radau-projection operator $\mathcal{I}_{V_p^s} = \mathbb{R}_h^+$, as defined in Zhang & Shu (2010). For the Burgers equation, in contrast to the linear advection equation, the direction of transport of information depends on the state and we therefore select the Lax–Wendroff

numerical flux

$$\mathbf{G}(\mathbf{u}, \mathbf{v}) = \mathbf{f}(\mathbf{w}(\mathbf{u}, \mathbf{v})), \quad \mathbf{w}(\mathbf{u}, \mathbf{v}) = \frac{1}{2} \left((\mathbf{u} + \mathbf{v}) + \frac{\Delta t}{h} (\mathbf{f}(\mathbf{v}) - \mathbf{f}(\mathbf{u})) \right).$$

For the Burgers equation we use Gauss–Legendre interpolation of the initial data in our numerical experiments. We have also tried other interpolation and projection operators and all of them lead to the same scaling behavior of the space-time residual. The space, time and stochastic integrals are numerically evaluated by a Gauss–Legendre quadrature. For the time integration we use 8 points, in the physical space we use 25 points and in the stochastic space 80 points. In the following we will call $\|u(T, \cdot, \cdot) - u_h^{N_t}\|_{L^2((0,1) \times \Omega)}$ numerical error and we will plot the quantities $\mathcal{E}^{\text{st}}(T)$, $\mathcal{E}^{\text{stoch}}(T)$ and the numerical error as in Theorem 3.14 at the final computational time T . Moreover, we plot the experimental order of convergence (eoc).

REMARK 4.1

1. As already mentioned after Remark 3.13, for nonlinear hyperbolic equations the space-time residual is suboptimal (by one order) on the first time step. Indeed, we lose half an order of convergence in the (global) space-time residual, i.e. when the error is of order h^{p+1} the error estimator is of order $h^{p+1/2}$. This is due to a lack of compatibility between the projection/interpolation of the initial data into the DG space and the spatial reconstruction. For the linear advection equation, where we compute the numerical solution using an upwind numerical flux, the Radau projection is the compatible choice, as it accounts for the upwind direction. Indeed, we have used it in our numerical experiments and observed optimal rates for the error estimator. A similar concept for nonlinear equations is up to now missing.
2. If we start to reconstruct the numerical solution of the Burgers equation from $t = 0$, we lose half an order of convergence in the space-time residual. Therefore, we start to reconstruct the numerical solution after the first time step on the coarsest mesh used for our computations. This corresponds to $t = 0.008$. We also start to integrate the space-time residual from $t = 0.008$ and obtain the full order of convergence in the space-time residual.

4.1 The linear advection equation

We consider the linear advection equation $\partial_t u + 2\partial_x u = 0$ on the spatial domain $[0, 2]_{\text{per}}$ and with $T = 0.2$. We start the computation with 16 elements and a time step-size of $\Delta t = 0.02$. We then subsequently reduce h and Δt by a factor of 2. The initial condition is given by $u^0(x, \xi) = \xi(1 - 0.5 \cos(\pi x))$, where we assume $\xi \sim \mathcal{U}[1, 3]$ to be uniformly distributed. In Figs 1 and 2 we show the numerical error between the exact solution $u(t, x, \xi) = \xi(1 - 0.5 \cos(\pi(x - 2t)))$ and the numerical solution computed by the Runge–Kutta DG method for 1 and 3 chaos polynomials ($N = 0, 2$), evaluated at $t_n = T$. Thanks to $C_{f''} = 0$ in this special case, the exponential term of the error indicator from Theorem 3.14 vanishes. In Fig. 1 we can see that the numerical error is not decreasing when h tends to zero. This is due to the term $\mathcal{E}_0^{\text{stoch}}$, cf. Remark 3.13. The overall error is dominated by the error we make in projecting the initial condition onto $\text{span}\{\Psi_0\}$. If we increase the number of orthonormal polynomials to 3, we obtain an exact representation of the initial condition in the orthonormal basis, i.e. $\mathcal{E}_0^{\text{stoch}} = 0$. Therefore, the numerical error consists of the space-time discretization error only, quantified by \mathcal{E}^{st} ; this can be seen in Fig. 2. After increasing the polynomial chaos degree, the numerical error decreases with the same order as the spatial residual. Furthermore, for $p = 1, 2$ both residuals have the correct order of convergence, i.e. $p + 1$.

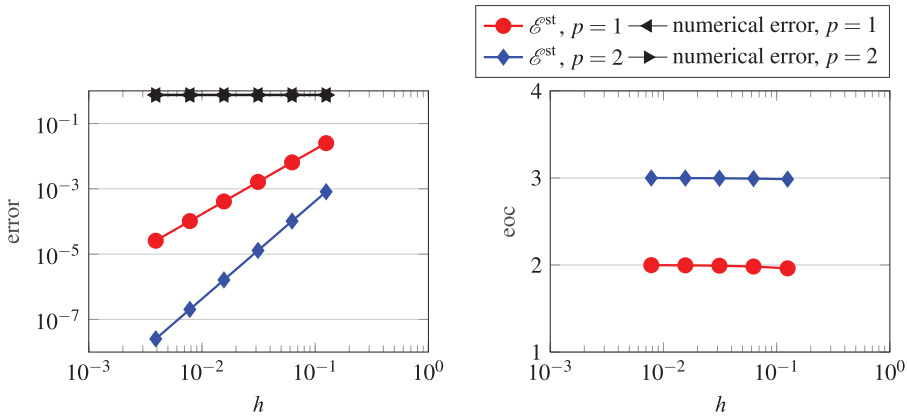


FIG. 1. Error and eoc plot for the linear advection equation in the case of 1 orthonormal polynomial and DG polynomial degrees $p = 1, 2$.

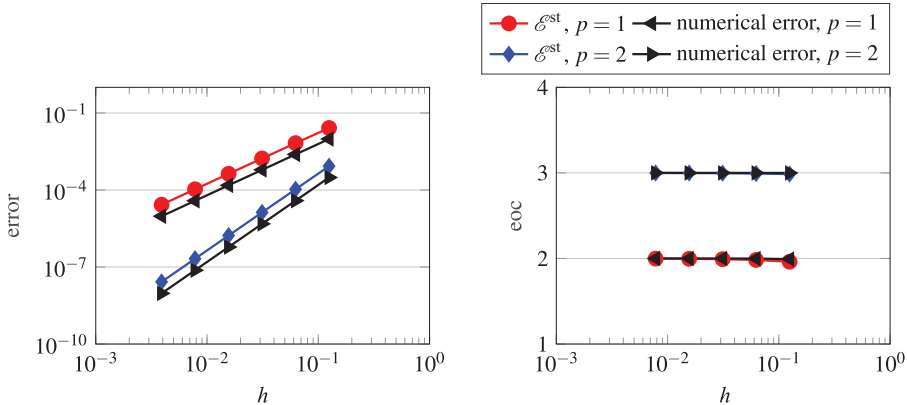


FIG. 2. Error and eoc plot for the linear advection equation in the case of 3 orthonormal polynomials and DG polynomial degrees $p = 1, 2$.

4.2 The Burgers equation with smooth solution

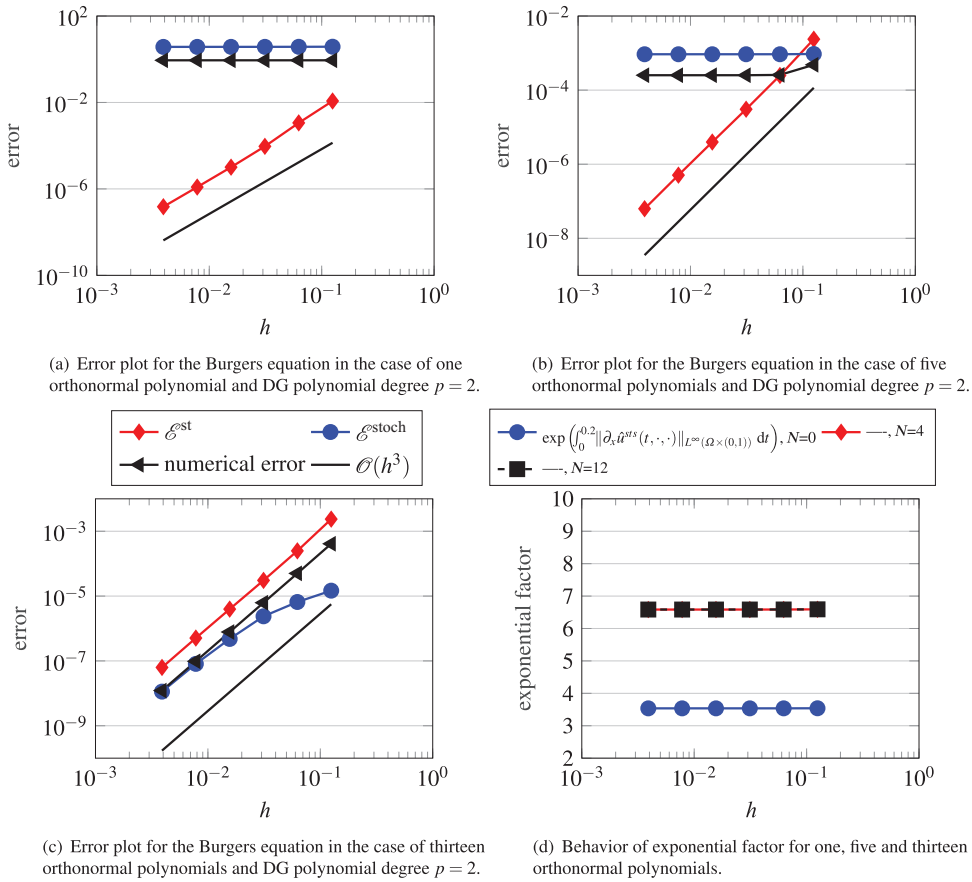
In this numerical example we consider the Burgers equation $\partial_t u + \partial_x(\frac{u^2}{2}) = S$ with the source term

$$S(t, x, \xi) = \pi \xi^2 \sin(\pi(x - \xi t)) (\cos(\pi(x - \xi t)) - 1),$$

$\xi \sim \mathcal{U}[1, 3]$. For the initial condition $u^0(x, \xi) = \xi \cos(\pi x)$, the exact solution for the Burgers equation is given by

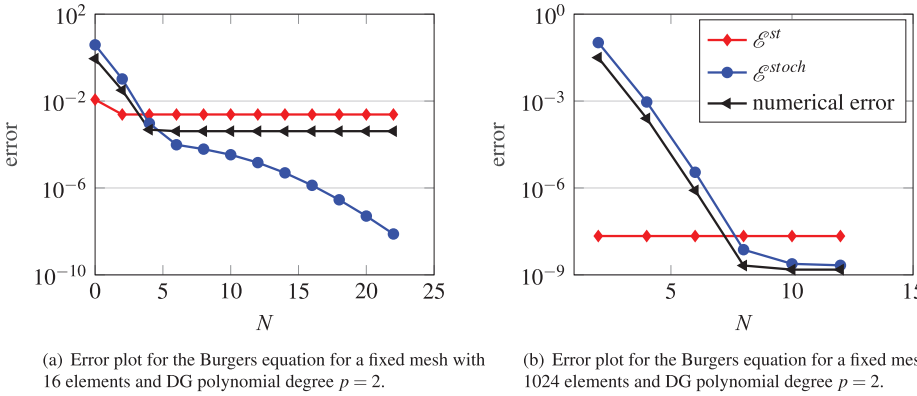
$$u(t, x, \xi) = \xi \cos(\pi(x - \xi t)).$$

The numerical solution is computed up to time $T = 0.2$ on the spatial domain $[0, 2]_{\text{per}}$ and we start the computations initially on a mesh with 16 elements and time step size $\Delta t = 0.008$. Again we reduce h and Δt by a factor of 2. The DG polynomial degree is 2 and the reconstruction in time is of order 3. In

FIG. 3. Error plots for the Burgers equation for h -refinement.

the following numerical computations we consider different cases, where on the one hand we refine the physical space and on the other hand we increase the polynomial degree of the orthonormal polynomials. The latter corresponds to a refinement in the stochastic space.

We start our computations by considering mesh refinements in the physical space with a fixed polynomial chaos degree. In Fig. 3(a) we display the numerical solution using only 1 chaos polynomial, which corresponds to $N = 0$. We can see that the numerical error is clearly dominated by $\mathcal{E}^{\text{stoch}}$. To reduce the overall error significantly we have to increase the polynomial chaos degree. We increase the number of polynomials to 5, corresponding to $N = 4$. We observe in Fig. 3(b) that for the coarse space discretization with 16 elements the numerical error is dominated by \mathcal{E}^{st} . However, after this point any significant reduction of the numerical error requires again an increase of the polynomial chaos degree as the numerical error is then again dominated by $\mathcal{E}^{\text{stoch}}$. When increasing the polynomial degree to 13 ($N = 12$) we can see in Fig. 3(c) that the numerical error is now dominated by \mathcal{E}^{st} , as the stochastic discretization is fine enough. The numerical error now converges with the same rate as the space-time residual. Additionally, in Fig. 3(d) we plot the exponential factor from Theorem 3.14 for different polynomial degrees N and different mesh sizes h . We can see that in the smooth case the

FIG. 4. Error plots for the Burgers equation for N -refinement.

exponential factor stays bounded for $h \rightarrow 0$. The exponential factor for $N = 0$ is smaller than for $N = 4, 12$ because we solve the (SG)-system only for the mean value.

In the previous computations we considered spatial refinements for a fixed polynomial chaos degree. Now we want to examine the behavior of $\mathcal{E}^{\text{stoch}}$ for different mesh sizes and a DG polynomial of degree 2. In Fig. 4(a) we show results for a fixed spatial discretization with 16 elements. We can see that the numerical error is dominated by \mathcal{E}^{st} , because the spatial discretization is too coarse. We can also see that \mathcal{E}^{st} remains unchanged by increasing the polynomial chaos degree. Additionally, we note that $\mathcal{E}^{\text{stoch}}$ exhibits spectral convergence. To reduce the numerical error we therefore need to increase the number of spatial elements or the DG polynomial degree. Finally, in Fig. 4(b) we consider a very fine mesh, consisting of 1024 elements. Due to the fine resolution of the physical space, the numerical error is dominated by $\mathcal{E}^{\text{stoch}}$ up to $N = 8$. After that point, the numerical error can be significantly decreased only by performing a spatial refinement. We can now also see how the numerical error converges spectrally until its convergence is again dominated by the spatial error.

Let us note that the spectral convergence of $\mathcal{E}^{\text{stoch}}$ is in accordance with what is known theoretically for stochastic discretization errors in SG schemes. Indeed, the authors of Gottlieb & Xiu (2008) prove spectral convergence of the SG method for the linear transport equation with random transport velocity. This indicates that the stochastic residual allows us to assess the magnitude of the stochastic discretization error in an optimal (spectral) way.

4.3 The Burgers equation, the artificial shock case

We study now the same example as in the previous section, but we compute numerical solutions up to $T = 0.56$ and use the slope limiter $\Lambda \Pi_h$ from Cockburn & Shu (2001). It is a well-known drawback of the SG-methodology, cf. the numerical example in Pettersson *et al.* (2015, Section 6), that even if the solution to (RIVP) is smooth up to time T , the solutions of the (SG)-system may develop discontinuities before that time. Indeed, this is the case in the example at hand. In Fig. 5(a) we display the numerical solutions and residuals for $N = 1$ at time T . The solution of the zeroth mode u_0 appears to contain a shock at approximately $x \approx 1.6$. We see that the spatial discontinuity is clearly picked up by the zeroth mode \mathbf{R}_0^{st} of the spatial residual and, to some extent, also in the second mode $\mathbf{R}_2^{\text{stoch}}$ of the stochastic residual. We may therefore use the spatial residual as an indicator for local spatial mesh refinements,

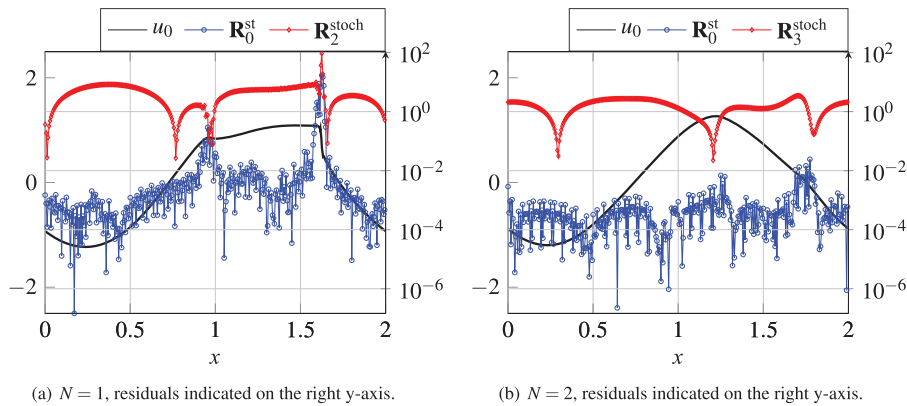


FIG. 5. Plot of the numerical solution, spatial residual and stochastic residual for the Burgers equation in the case of 2 and 3 orthonormal polynomials and DG polynomial degree $p = 2$.

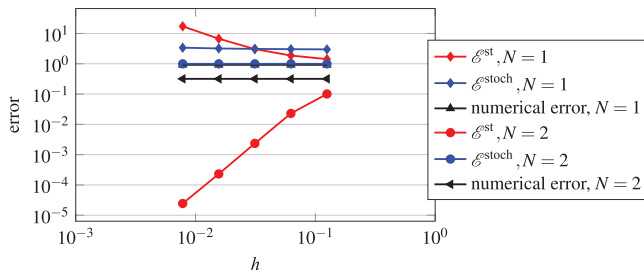


FIG. 6. Comparison of residuals and numerical error for 1 and 2 orthonormal polynomials and DG polynomial degree $p = 2$.

which will be left to future research. Moreover, we can see in Fig. 6 that for $h \rightarrow 0$ the spatial residual blows up, although the numerical error stays constant. Also $\mathcal{E}^{\text{stoch}}$ grows with $h \rightarrow 0$, although very slowly compared to \mathcal{E}^{st} . Increasing the polynomial chaos degree to $N = 2$ also increases the smoothness of the numerical solution, which can be seen in Fig. 5(b). In Fig. 6 we can see that for $N = 2$, \mathcal{E}^{st} decreases when $h \rightarrow 0$.

The artificial generation of shocks is a general problem of the SG method; however, our residuals were able to detect the position of the shock correctly. This demonstrates that our error estimator picks up on the ‘artificial’ discontinuity and can help the user to determine a more suitable polynomial degree in which no such discontinuities are present. It should be noted, however, that the estimator cannot distinguish between discontinuities in the solution u of (RIVP) and ‘artificial’ discontinuities in the solution of the (SG)-system. Furthermore, there are cases in which the ‘artificial’ discontinuities cannot be avoided as easily as in the example at hand. In one example in Pettersson *et al.* (2015, Section 6) each (SG)-solution contains shocks and for increasing N the number of shocks increases while their size decreases. From the numerical point of view (for some fixed $h > 0$) a solution with very small shocks cannot be distinguished from a smooth solution. In such a case it is probably possible to obtain a sequence of approximate solutions for which the error estimator converges by choosing h and N such that they are properly related, but a detailed discussion of this issue is beyond the scope of this work.

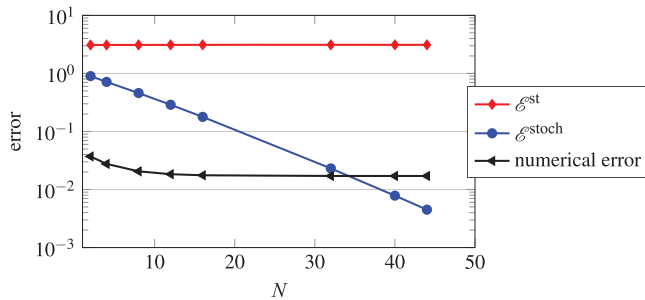


FIG. 7. Error plot for the Burgers equation for a fixed mesh with 512 elements and DG polynomial degree $p = 2$.

4.4 The Burgers equation, the shock case

As final numerical example, we consider a Riemann problem for the Burgers equation, where the jump size of the discontinuity, and thus the shock speed, is random. The spatial domain is now $[-1, 1]$ and we set $T = 0.1$. The initial condition is given by

$$u^0(x, \xi) = \begin{cases} 1 + \xi & \text{if } x \leq 0, \\ 0.5 + \xi & \text{otherwise,} \end{cases}$$

where $\xi \sim \mathcal{U}[-0.2, 0.2]$. The shock speed can be computed as $s(\xi) = 1.5 + 2\xi$ and therefore the exact solution for the Burgers equation is given by

$$u(t, x, \xi) = \begin{cases} 1 + \xi & \text{if } x \leq s(\xi)t, \\ 0.5 + \xi & \text{otherwise.} \end{cases}$$

As the shock speed is \mathbb{P} -a.s. positive we use the upwind numerical flux in this numerical experiment. We use the slope limiter $\Lambda \Pi_h$ from Cockburn & Shu (2001) and consider a very fine physical resolution with 512 elements and DG polynomial degree of 2. Although the exact solution is discontinuous we can see in Fig. 7 that $\mathcal{E}^{\text{stoch}}$ exhibits exponential convergence for a sufficiently large number of orthonormal polynomials. This is due to the fact that the coefficients of u in the polynomial chaos expansion are smooth; cf. Pettersson *et al.* (2015, Section 6). Hence, although the exact solution is discontinuous $\mathcal{E}^{\text{stoch}}$ displays the correct (spectral) type of convergence and, moreover, it gives us information about the resolution in the stochastic space independent of the spatial resolution.

5. Conclusions

This work provides a first rigorous *a posteriori* error analysis of scalar conservation laws with uncertain initial conditions and source terms. We derived an *a posteriori* error estimator for the random conservation law and additionally showed that the space-time stochastic residual admits an orthogonal splitting into a residual representing the space-time error and a residual representing the stochastic error. Numerical experiments demonstrate that the two parts of the error estimator scale in N and h as expected. Moreover, in the case of the linear advection equation, the space-time residual exhibits the

optimal order of convergence. Furthermore, the numerical experiments showed that both residuals serve as indicators to determine whether, after a completed computation, one should increase the polynomial chaos degree or perform a spatial refinement to decrease the overall numerical error. In the case of a spatial discontinuity, the discontinuity is also visible in the stochastic residual.

Future work will focus on the *a posteriori* error analysis of systems of conservation laws with uncertain initial conditions or uncertain parameters, for example for the Euler equations. Due to the relative entropy framework we expect our theory to be extendable to this case. Additionally, our approach can also be applied to scalar conservation laws with random flux functions, as for example in Mishra *et al.* (2016). For further applications of our method, the construction of space–stochastic adaptive schemes using the hybrid SG method (Bürger *et al.*, 2014) and the residuals as local indicators will be considered.

Funding

Baden-Württemberg Stiftung via the project ‘Numerical Methods for Multiphase Flows with Strongly Varying Mach Numbers’ (to J.G.); project ‘SEAL’ (to F.M., C.R.).

REFERENCES

- ABGRALL, R. & MISHRA, S. (2017) *Uncertainty Quantification for Hyperbolic Systems of Conservation Laws*, Chapter 19. Amsterdam: Elsevier.
- BIJL, H., LUCOR, D., MISHRA, S. & SCHWAB, C. (2013) *Uncertainty Quantification in Computational Fluid Dynamics*. Lecture Notes in Computational Science and Engineering, vol. 92. Heidelberg: Springer, pp. xii+333.
- BÜRGER, R., KRÖKER, I. & ROHDE, C. (2014) A hybrid stochastic Galerkin method for uncertainty quantification applied to a conservation law modelling a clarifier-thickener unit. *Z. Angew. Math. Mech.*, **94**, 793–817.
- BUTLER, T., DAWSON, C. & WILDEY, T. (2011) A posteriori error analysis of stochastic differential equations using polynomial chaos expansions. *SIAM J. Sci. Comput.*, **33**, 1267–1291.
- COCKBURN, B. (2003) Continuous dependence and error estimation for viscosity methods. *Acta Numerica*, **12**, 127–180.
- COCKBURN, B. & SHU, C.-W. (1998) The Runge–Kutta discontinuous Galerkin method for conservation laws V: Multidimensional systems. *J. Comput. Phys.*, **141**, 199–224.
- COCKBURN, B. & SHU, C.-W. (2001) Runge–Kutta discontinuous Galerkin methods for convection-dominated problems. *J. Sci. Comput.*, **16**, 173–261.
- DAFERMOS, C. M. (2016) *Hyperbolic Conservation Laws in Continuum Physics*, 4th edn. Grundlehren der Mathematischen Wissenschaften [Fundamental Principles of Mathematical Sciences], vol. 325. Berlin: Springer, pp. xxxviii+826.
- DEB, M. K., BABUŠKA, I. M. & ODEN, J. T. (2001) Solution of stochastic partial differential equations using Galerkin finite element techniques. *Comput. Methods Appl. Mech. Eng.*, **190**, 6359–6372.
- DEDNER, A. & GIesselmann, J. (2016) A posteriori analysis of fully discrete method of lines discontinuous Galerkin schemes for systems of conservation laws. *SIAM J. Numer. Anal.*, **54**, 3523–3549.
- DEDNER, A., MAKRIDAKIS, C. & OHLBERGER, M. (2007) Error control for a class of Runge–Kutta discontinuous Galerkin methods for nonlinear conservation laws. *SIAM J. Numer. Anal.*, **45**, 514–538.
- DESPRÉS, B., POËTTE, G. & LUCOR, D. (2013) Robust uncertainty propagation in systems of conservation laws with the entropy closure method. *Uncertainty Quantification in Computational Fluid Dynamics*. Lecture Notes in Computational Science and Engineering, vol. 92. Heidelberg: Springer, pp. 105–149.
- EIGEL, M., GITTELSON, C. J., SCHWAB, C. & ZANDER, E. (2014) Adaptive stochastic Galerkin FEM. *Comput. Methods Appl. Mech. Eng.*, **270**, 247–269.

- ERDÉLYI, A., MAGNUS, W., OBERHETTINGER, F. & TRICOMI, F. G. (1981) *Higher Transcendental Functions*, vol. 2. Melbourne, FL: Robert E. Krieger, pp. xviii+396. Based on notes left by Harry Bateman, reprint of the 1953 original.
- GEORGULIS, E. H., HALL, E. & MAKRIDAKIS, C. (2014) Error control for discontinuous Galerkin methods for first order hyperbolic problems. *Recent Developments in Discontinuous Galerkin Finite Element Methods for Partial Differential Equations*. IMA Volumes in Mathematics and its Applications, vol. 157. Cham: Springer, pp. 195–207.
- GHANEM, R. G. & SPANOS, P. D. (1991) *Stochastic Finite Elements: A Spectral Approach*. New York: Springer, pp. x+214.
- GIESSELMANN, J., MAKRIDAKIS, C. & PRYER, T. (2015) A posteriori analysis of discontinuous Galerkin schemes for systems of hyperbolic conservation laws. *SIAM J. Numer. Anal.*, **53**, 1280–1303.
- GOSSE, L. & MAKRIDAKIS, C. (2000) Two a posteriori error estimates for one-dimensional scalar conservation laws. *SIAM J. Numer. Anal.*, **38**, 964–988.
- GOTTLIEB, D. & XIU, D. (2008) Galerkin method for wave equations with uncertain coefficients. *Commun. Comput. Phys.*, **3**, 505–518.
- HINDENLANG, F., GASSNER, G. J., ALTMANN, C., BECK, A., STAUDENMAIER, M. & MUNZ, C.-D. (2012) Explicit discontinuous Galerkin methods for unsteady problems. *Comput. Fluids*, **61**, 86–93.
- HOANG, V. H. & SCHWAB, C. (2013) Sparse tensor Galerkin discretization of parametric and random parabolic PDEs—analytic regularity and generalized polynomial chaos approximation. *SIAM J. Math. Anal.*, **45**, 3050–3083.
- HU, J., JIN, S. & XIU, D. (2015) A stochastic Galerkin method for Hamilton-Jacobi equations with uncertainty. *SIAM J. Sci. Comput.*, **37**, A2246–A2269.
- JIN, S. & MA, Z. (2018) The discrete stochastic Galerkin method for hyperbolic equations with non-smooth and random coefficients. *J. Sci. Comp.*, **74**, 97–121.
- KÖPPEL, M., KRÖKER, I. & ROHDE, C. (2017) Intrusive uncertainty quantification for hyperbolic-elliptic systems governing two-phase flow in heterogeneous porous media. *Comput. Geosci.*, **21**, 807–832.
- KRÖKER, I., NOWAK, W. & ROHDE, C. (2015) A stochastically and spatially adaptive parallel scheme for uncertain and nonlinear two-phase flow problems. *Comput. Geosci.*, **19**, 269–284.
- KRÖNER, D. & OHLBERGER, M. (2000) A posteriori error estimates for upwind finite volume schemes for nonlinear conservation laws in multidimensions. *Math. Comput.*, **69**, 25–39.
- KRUŽKOV, S. N. (1970) First order quasilinear equations with several independent variables. *Mat. Sb. (N.S.)*, **81**, 228–255.
- LE MAÎTRE, O. P. & KNIO, O. M. (2010) *Spectral Methods for Uncertainty Quantification: With Applications to Computational Fluid Dynamics*. New York: Springer, pp. xvi+536.
- LE MAÎTRE, O. P., KNIO, O. M., NAJM, H. N. & GHANEM, R. G. (2004) Uncertainty propagation using Wiener–Haar expansions. *J. Comput. Phys.*, **197**, 28–57.
- MATHELIN, L. & LE MAÎTRE, O. P. (2007) Dual-based a posteriori error estimate for stochastic finite element methods. *Comm. App. Math. Comp. Sci.*, **2**, 83–115.
- MISHRA, S., RISEBRO, N. H., SCHWAB, C. & TOKAREVA, S. (2016) Numerical solution of scalar conservation laws with random flux functions. *SIAM/ASA J. Uncertain. Quantif.*, **4**, 552–591.
- MISHRA, S. & SCHWAB, C. (2012) Sparse tensor multi-level Monte Carlo finite volume methods for hyperbolic conservation laws with random initial data. *Math. Comput.*, **81**, 1979–2018.
- MÜLLER, S. (2003) *Adaptive Multiscale Schemes for Conservation Laws*. Lecture Notes in Computational Science and Engineering, vol. 27. Berlin, Springer, pp. xiv+181.
- PETTERSSON, M. P., IACCARINO, G. & NORDSTRÖM, J. (2015) *Polynomial Chaos Methods for Hyperbolic Partial Differential Equations: Numerical Techniques for Fluid Dynamics Problems in the Presence of Uncertainties*. Cham: Springer, pp. xii+214.
- PULTAROVÁ, I. (2015) Adaptive algorithm for stochastic Galerkin method. *Appl. Math.*, **60**, 551–571.
- TOULORGE, T. & DESMET, W. (2012) Optimal Runge–Kutta schemes for discontinuous Galerkin space discretizations applied to wave propagation problems. *J. Comput. Phys.*, **231**, 2067–2091.

- TRYOEN, J., LE MAÎTRE, O. P. & ERN, A. (2012) Adaptive anisotropic spectral stochastic methods for uncertain scalar conservation laws. *SIAM J. Sci. Comput.*, **34**, A2459–A2481.
- WAN, X. & KARNIADAKIS, G. E. (2006) Multi-element generalized polynomial chaos for arbitrary probability measures. *SIAM J. Sci. Comput.*, **28**, 901–928.
- WIENER, N. (1938) The homogeneous chaos. *Amer. J. Math.*, **60**, 897–936.
- XIU, D. & KARNIADAKIS, G. E. (2002) The Wiener–Askey polynomial chaos for stochastic differential equations. *SIAM J. Sci. Comput.*, **24**, 619–644.
- YAN, Y. (2005) Galerkin finite element methods for stochastic parabolic partial differential equations. *SIAM J. Numer. Anal.*, **43**, 1363–1384.
- ZHANG, Q. & SHU, C.-W. (2010) Stability analysis and a priori error estimates of the third order explicit Runge–Kutta discontinuous Galerkin method for scalar conservation laws. *SIAM J. Numer. Anal.*, **48**, 1038–1063.
- ZHOU, T. & TANG, T. (2012) Convergence analysis for spectral approximation to a scalar transport equation with a random wave speed. *J. Comput. Math.*, **30**, 643–656.